Downlink Transmit Design in Massive MIMO LEO Satellite Communications

Ke-Xin Li, *Student Member, IEEE,* Li You, *Member, IEEE,*
Jiaheng Wang, *Senior Member, IEEE,* Xiqi Gao, *Fellow, IEEE,*
Christos G. Tsinos, *Senior Member, IEEE,*
Symeon Chatzinotas, *Senior Member, IEEE,* and Björn Ottersten, *Fellow, IEEE*

Abstract

Low earth orbit (LEO) satellite communication systems have attracted extensive attention due to their smaller pathloss, shorter round-trip delay and lower launch cost compared with geostationary counterparts. In this paper, the downlink transmit design for massive multiple-input multiple-output (MIMO) LEO satellite communications is investigated. First, we establish the massive MIMO LEO satellite channel model where the satellite and user terminals (UTs) are both equipped with the uniform planar arrays. Then, the rank of transmit covariance matrix of each UT is shown to be no larger than one to maximize ergodic sum rate, which reveals the optimality of single-stream precoding for each UT. The minorization-maximization algorithm is used to compute the precoding vectors. To reduce the computation complexity, an upper bound of ergodic sum rate is resorted to produce a simplified transmit design, where the rank of optimal transmit covariance matrix of each UT is also shown to not exceed one. To tackle the simplified precoder design, we derive the structure of precoding vectors, and formulate a Lagrange multiplier optimization (LMO) problem building on the structure. Then, a low-complexity algorithm is devised to solve the LMO, which takes much less computation effort. Simulation results verify the performance of proposed approaches.

Index Terms

Satellite communications, massive MIMO, DL transmit design, LEO.

K.-X. Li, L. You, J. Wang and X. Q. Gao are with the National Mobile Communications Research Laboratory, Southeast University, Nanjing 210096, China (e-mail: likexin3488@seu.edu.cn, liyou@seu.edu.cn, jhwang@seu.edu.cn, xqgao@seu.edu.cn). C. G. Tsinos, S. Chatzinotas and B. Ottersten are with the Interdisciplinary Centre for Security, Reliability and Trust (SnT), University of Luxembourg, Luxembourg City 2721, Luxembourg (e-mail: chtsinos@gmail.com, symeon.chatzinotas@uni.lu, bjorn.ottersten@uni.lu).*(Corresponding author: Xiqi Gao)*

I. INTRODUCTION

The ever increasing data demand makes more stringent requirements for the future wireless network, which is expected to have high throughput, global and seamless coverage, reliability, and massive connectivity [1]. As a critical enabler to achieve this ambitious target, satellite communications (SATCOM) can provide continuous and ubiquitous connectivity for areas where there is no or inadequate Internet access [2]. In recent years, low earth orbit (LEO) satellites typically deployed between 500 km and 2000 km from the earth have attracted intensive research interest due to their less pathloss, shorter round-trip delay and lower launch cost, with respect to the geostationary earth orbit (GEO) opponents [3]–[6]. Up to now, several projects have been started by the governments and corporations to develop LEO SATCOM, e.g., Iridium, Globalstar, OneWeb, Starlink, Telesat, Hongyun [7].

Multiple-input multiple-output (MIMO) has been a crucial technique to make the best of the scarce spectrum in SATCOM. Generally, the study of MIMO over SATCOM can be divided into two categories: single-user case and multi-user case. In single-user case, MIMO channel can be built by using dual polarization antennas [8]–[10], multiple earth stations [8], [11], multiple satellites [8], [12], etc. For multi-user case, plenty of user terminals (UTs) are usually served by the multibeam satellite.

Multibeam satellites play an important role in SATCOM, which divide the coverage area into small regions via spot beams [13]. Basically, the spot beams can be generated by using the multifeed reflector antennas or phased-array antennas (PAAs)[1] at the satellite [15]. The GEO satellites usually employ the multifeed reflector antennas [16]. Meanwhile, the LEO satellites prefer to use the PAAs because of their wide-angle scanning requirements [15], e.g., Globalstar [17] and Starlink [7]. In current satellite systems, multiple color reuse scheme is often adopted to suppress co-channel interference by exploiting different frequency bands and orthogonal polarizations [18]. As a result, the frequency bands can be reused among sufficiently isolated beams, and the system capacity will increase substantially. To exploit the limited spectrum more aggressively, the full frequency reuse (FFR) scheme has been proposed, in which all the beams share the frequency bands [19], [20]. However, advanced techniques are indispensable to manage inter-beam interference for FFR scheme.

[1]For PAAs, the phase shifters in the beamforming network can be agilely controlled to produce multiple beams [14].

Serious co-channel interference can be alleviated by meticulous transmit design [11], [21]–[26]. A generic precoding approach for a class of objective functions and power constraints is presented in [21] for multibeam satellite systems. Based on the superframe structure in the DVB-S2X standard, the multi-group multicasting principle has been incorporated in the precoding for frame-based multibeam satellites [22], [23], [25], [26]. The distributed precoding for multi-gateway multibeam satellites can be found in [23], [24], [26]. In [11], the antenna geometry in the MIMO feeder link and zero-forcing (ZF) precoder in the multibeam downlink (DL) are jointly designed.

The performance of precoding relies severely on the quality of channel state information (CSI) at the transmitter. The aforementioned works on precoding in multibeam satellites assume that the transmitter can track instantaneous CSI (iCSI) [11], [21]–[27]. In LEO SATCOM, the intrinsic channel impairments, e.g., large Doppler shifts and propagation delays, will render it difficult to acquire iCSI at the transmitter (iCSIT). In more detail, for time-division duplexing (TDD) systems, the estimated uplink (UL) iCSI is directly used for DL transmission, which would be outdated after the DL transmit signals arrive at ground UTs. In frequency-division duplexing (FDD) systems, the DL iCSI is estimated at each UT and then fed back to the satellite, which could bring considerable training and feedback overhead. Moreover, the feedback would also be outdated due to the large delays. In contrast to iCSI, statistical CSI (sCSI) can keep stable for longer time intervals [28], [29], which makes it easier to be acquired at the transmitter. Hence, in this paper, we assume that only sCSI is known at the satellite to perform DL transmit design.

Massive MIMO has been one of the fundamental techniques in terrestrial 5G communications, where the base station (BS) equipped with a large number of antennas serves tens of UTs simultaneously [30]. With substantial degrees of freedom in the spatial domain, massive MIMO is capable of achieving higher spectral efficiency and energy efficiency [31]. The application of massive MIMO in SATCOM is envisioned to be a promising solution of future wideband satellite systems [32]. The DL fixed multibeam selection and radio resource management with multiple color reuse are jointly considered in [33] for massive MIMO SATCOM. In this paper, we study the DL transmit design in FFR massive MIMO LEO SATCOM, where a large number of antennas are deployed at the LEO satellite. For fully digital-implemented satellites, it is unnecessary to adopt predefined multiple beamforming [32]. By means of the massive MIMO technique, the restriction of using fixed multiple beamforming in multibeam satellites may be removed.

Up to now, there are abundant works on DL transmit designs in massive MIMO terrestrial wireless communications with sCSI at the transmitter (sCSIT), e.g., two-stage precoder design [34], beam domain transmission [35], and robust precoder design [36]. In the two-stage precoder design [34], the out-layer precoding suppresses interferences between UT groups by using the sCSI, while the inner-layer precoding provides spatial multiplexing for intra-group UTs by adapting to the effective iCSI with reduced dimension. In the beam domain transmission [35], the BS communicates with different UTs on non-overlapping beams by exploiting beam domain sCSI. In [36], the robust precoder design and its low-complexity implementation are investigated by considering a posteriori channel model after UL channel training. However, the approaches in aforementioned works may not apply to LEO SATCOM due to the unavailability of special LEO satellite channel characteristics and high implementation complexity for limited satellite payloads. Recently, a transmission approach for massive MIMO LEO SATCOM is proposed in [37], where the channel model, closed-form DL precoders and UL receivers, and user grouping strategy are investigated. In [37], each UT is assumed to have a single antenna, and the DL precoders therein are calculated by maximizing the average signal-to-leakage-plus-noise ratio (ASLNR).

In this paper, we investigate the DL transmit design in massive MIMO LEO SATCOM by maximizing the ergodic sum rate, where the satellite and UTs use the uniform planar arrays (UPAs). Since multiple antennas are deployed at each UT, it is of great importance to know the maximum data streams that can be delivered to each UT. Our major contributions are summarized as follows:

- We show that the rank of optimal transmit covariance matrix of each UT is no larger than one to maximize the ergodic sum rate, which implies that single-stream precoding for each UT is optimal for linear transmitters even though each UT has multiple antennas. The optimal linear receiver of each UT is also derived. Since the ergodic sum rate is a non-convex function and involves mathematical expectations, it is generally difficult to be maximized. The minorization-maximization (MM) algorithm combined with Monte-Carlo method is adopted to obtain a locally optimal solution to the DL precoder design.
- To reduce the computation compleixty in Monte-Carlo method, we simplify the DL transmit design by using an upper bound of the ergodic sum rate. We show that the transmit covariance matrices with rank no larger than one are also optimal. To tackle the simplified precoder design, the structure of precoders is derived, which indicates that the precoders

are only determined by the same number of scalar Lagrange multipliers as UTs. Then, a Lagrange multiplier optimization (LMO) problem is formulated, where only one scalar Lagrange multiplier rather than a precoding vector needs to be optimized for each UT. Besides, the LMO problem is shown to be equivalent to the power allocation (PA) problem in a virtual UL, and a low-complexity algorithm is presented to solve the virtual UL PA problem, which requires much less computation effort.

The remainder of this paper is organized as follows. Section II introduces the system model, where the channel model is presented for the satellite and UTs equipped with the UPAs. Section III shows the rank property of transmit covariances and MM algorithm is used to design the DL precoder. In Section IV, we formulate the simplified DL transmit design by using an upper bound of the ergodic sum rate. It is shown that the rank property of transmit covariance matrices still holds, and the corresponding simplified precoder optimization is transformed into the LMO. Section V provides simulation results. Section VI concludes this paper.

Notations: Throughout this paper, lower case letters denote scalars, and boldface lower (upper) letters denote vectors (matrices). The set of all n-by-m complex (real) matrices is denoted as $\mathbb{C}^{n\times m}$ ($\mathbb{R}^{n\times m}$). $\mathrm{tr}(\cdot)$, $\det(\cdot)$, $\mathrm{rank}(\cdot)$, $(\cdot)^*$, $(\cdot)^T$, and $(\cdot)^H$ denote the trace, determinant, rank, conjugate, transpose, and conjugate transpose operation for matrix argument, respectively. $|\cdot|$ denotes the absolute value. The Euclidean norm of vector $\mathbf{x}$ is denoted as $\|\mathbf{x}\| = \sqrt{\mathbf{x}^H\mathbf{x}}$. The Frobenius norm of matrix $\mathbf{A}$ is denoted as $\|\mathbf{A}\|_{\mathrm{F}} = \sqrt{\mathrm{tr}(\mathbf{A}^H\mathbf{A})}$. $\otimes$ denotes the Kronecker product. $[\mathbf{A}]_{n,m}$ denotes the (n,m)th element of matrix $\mathbf{A}$. $\mathrm{diag}(\mathbf{a})$ denotes the diagonal matrix with $\mathbf{a}$ along its main diagonal. $\mathbb{E}\{\cdot\}$ denotes mathematical expectation. $\mathcal{CN}(\mathbf{0},\mathbf{C})$ denotes the circular symmetric complex Gaussian random vector with zero mean and covariance $\mathbf{C}$. $\mathrm{U}\ [a,b]$ represents the uniform distribution between a and b. $\triangleq$ denotes "be defined as". $\sim$ denotes "be distributed as".

II. System Model

A. System Setup

We consider the DL transmission in FFR massive MIMO LEO SATCOM over lower frequency bands, e.g., L/S/C bands. The mobile UTs are served under the footprint of a single LEO satellite as shown in Fig. 1. The satellite is supposed to work with a regenerative payload, which allows on-board processing (OBP) of baseband signals on satellites [20]. The satellite and mobile UTs are equipped with the UPAs, the amplitude and phase on each antenna element of which can

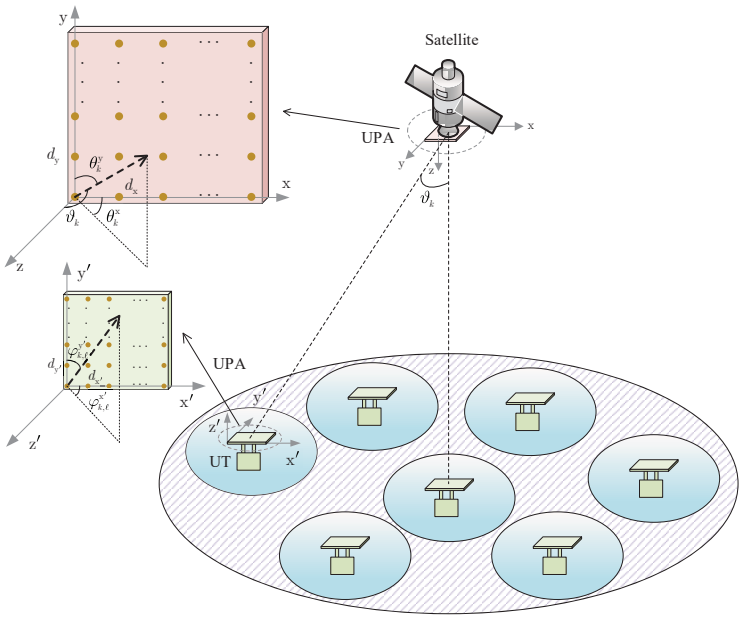

Fig. 1: The DL in FFR massive MIMO LEO SATCOM.

be digitally controlled. The satellite has the large-scale UPA with M_{x} and M_{y} elements in the x-axis and y-axis, respectively. The total number of antennas at the satellite is $M_{\mathrm{x}}M_{\mathrm{y}} \triangleq M$. Considering that the UTs under service are located in a small part of the visual range seen at the satellite, each antenna element of the UPA at the satellite is assumed to be directional. On the other hand, each UT uses the UPA consisting of $N_{\mathrm{x}'}$ and $N_{\mathrm{y}'}$ omnidirectional elements in the x$'$-axis and y$'$-axis, respectively, and the total number of antennas at each UT is $N_{\mathrm{x}'}N_{\mathrm{y}'} \triangleq N$. The approaches in this paper can be directly extended to the case where the UPAs at UTs have different numbers of antenna elements.

B. DL Channel Model

The DL LEO satellite channel model is introduced as follows. The DL channel matrix $\check{\mathbf{H}}_k(t,f) \in \mathbb{C}^{N\times M}$ between LEO satellite and UT k at time instant t and frequency f can be represented by

$$\check{\mathbf{H}}_k(t,f) = \sum_{\ell=0}^{L_k-1} a_{k,\ell} e^{j2\pi\left(\nu_{k,\ell}t - f\tau_{k,\ell}\right)} \mathbf{d}_{k,\ell} \cdot \mathbf{g}_{k,\ell}^H, \tag{1}$$

where $j \triangleq \sqrt{-1}$, L_k is the multipath number of UT k's channel, $a_{k,\ell}$, $\nu_{k,\ell}$ and $\tau_{k,\ell}$ are the complex channel gain, Doppler shift and propagation delay for the ℓth path of UT k's channel. The vectors $\mathbf{d}_{k,\ell} \in \mathbb{C}^{N\times 1}$ and $\mathbf{g}_{k,\ell} \in \mathbb{C}^{M\times 1}$ in (1) are the array response vectors at the UT and satellite sides, respectively, which are associated with the ℓth path of UT k's channel.

For simplicity, we assume that the channel matrix $\check{\mathbf{H}}_k(t,f)$ is approximately stable within each coherence time interval, and changes from block to block according to some ergodic process. In the following, we will describe the LEO satellite channel characteristics one by one, which mainly include Doppler shifts, propagation delays, and array response vectors.

1) Doppler shifts: For LEO satellite channels, the Doppler shifts will be much larger compared with those in terrestrial wireless channels, due to the large relative velocity between satellite and UTs. At 2 GHz carrier frequency, the Doppler shift can be 40 kHz for LEO satellite at an altitude of 1000 km [38]. The Doppler shift $\nu_{k,\ell}$ for the ℓth path of UT k's channel mainly consists of two parts [39], i.e., $\nu_{k,\ell} = \nu_{k,\ell}^{\mathrm{sat}} + \nu_{k,\ell}^{\mathrm{ut}}$, where $\nu_{k,\ell}^{\mathrm{sat}}$ and $\nu_{k,\ell}^{\mathrm{ut}}$ are Doppler shifts relevant to the movement of satellite and UT k, respectively. The first part $\nu_{k,\ell}^{\mathrm{sat}}$, which is dominated in $\nu_{k,\ell}$, will be nearly identical for different paths of UT k's channel, because of the high altitude of satellite [39]. Hence, $\nu_{k,\ell}^{\mathrm{sat}}$ can be rewritten as $\nu_{k,\ell}^{\mathrm{sat}} = \nu_k^{\mathrm{sat}}$ for $0 \le \ell \le L_k - 1$. The variation of ν_k^{sat} with time behaves rather deterministically, and it can be estimated and compensated at each UT. Specifically, ν_k^{sat} can be expressed as $\nu_k^{\mathrm{sat}} = f_c(v_k/c)\cos\phi_k$ [38], where f_c is the carrier frequency, c is the speed of light, v_k is the velocity of satellite, and ϕ_k is the angle between satellite's forward velocity and boresight from satellite to UT k. On the other hand, the $\nu_{k,\ell}^{\mathrm{ut}}$'s are usually distinct for different paths.

2) Propagation Delays: For LEO satellites, the propagation delay is a more serious problem than that in terrestrial wireless channels, on account of the long distance between satellite and UTs. For LEO satellite at an altitude of 1200 km, the round trip time can be about 20 ms [4]. The minimal and maximal propagation delays of UT k's channel are represented by $\tau_k^{\min} = \min_\ell \tau_{k,\ell}$ and $\tau_k^{\max} = \max_\ell \tau_{k,\ell}$, respectively.

3) Array response vectors: Define $\boldsymbol{\theta}_{k,\ell} = (\theta_{k,\ell}^{\mathrm{x}}, \theta_{k,\ell}^{\mathrm{y}})$ and $\boldsymbol{\varphi}_{k,\ell} = (\varphi_{k,\ell}^{\mathrm{x}'}, \varphi_{k,\ell}^{\mathrm{y}'})$ as the paired angles-of-departure (AoDs) and angles-of-arrival (AoAs) for the ℓth path of UT k's channel, respectively. The array response vectors $\mathbf{g}_{k,\ell}$ and $\mathbf{d}_{k,\ell}$ in (1) are given by $\mathbf{g}_{k,\ell} = \mathbf{g}(\boldsymbol{\theta}_{k,\ell})$ and $\mathbf{d}_{k,\ell} = \mathbf{d}(\boldsymbol{\varphi}_{k,\ell})$, respectively, where $\mathbf{g}(\boldsymbol{\theta}) = \mathbf{a}_{M_{\mathrm{x}}}\left(\sin\theta_{\mathrm{y}}\cos\theta_{\mathrm{x}}\right) \otimes \mathbf{a}_{M_{\mathrm{y}}}\left(\cos\theta_{\mathrm{y}}\right)$ and $\mathbf{d}(\boldsymbol{\varphi}) = \mathbf{a}_{N_{\mathrm{x}'}}\left(\sin\varphi_{\mathrm{y}'}\cos\varphi_{\mathrm{x}'}\right) \otimes \mathbf{a}_{N_{\mathrm{y}'}}\left(\cos\varphi_{\mathrm{y}'}\right)$ for arbitrary $\boldsymbol{\theta} = (\theta_{\mathrm{x}}, \theta_{\mathrm{y}})$ and $\boldsymbol{\varphi} = (\varphi_{\mathrm{x}'}, \varphi_{\mathrm{y}'})$. The $\mathbf{a}_{n_{\mathrm{v}}}(\phi) \in \mathbb{C}^{n_{\mathrm{v}}\times 1}$ is expressed as $\mathbf{a}_{n_{\mathrm{v}}}(\phi) = \frac{1}{\sqrt{n_{\mathrm{v}}}}(1, e^{-j\frac{2\pi d_{\mathrm{v}}}{\lambda}\phi}, \ldots, e^{-j\frac{2\pi d_{\mathrm{v}}}{\lambda}(n_{\mathrm{v}}-1)\phi})^T$, where $\lambda = c/f_c$ is the carrier wavelength, d_{v} is the antenna spacing along v-axis with $\mathrm{v} \in \{\mathrm{x}, \mathrm{y}, \mathrm{x}', \mathrm{y}'\}$. In satellite channels, because the scattering on ground only takes place within a few kilometers around each UT, the AoDs for different paths of UT k's channel are nearly identical due to the long distance between satellite and UT k [37], i.e., $\boldsymbol{\theta}_{k,\ell} = \boldsymbol{\theta}_k$, $0 \le \ell \le L_k - 1$. Thus, we can rewrite

$\mathbf{g}_{k,\ell} = \mathbf{g}_k = \mathbf{g}(\boldsymbol{\theta}_k)$, where $\boldsymbol{\theta}_k = (\theta_k^{\mathrm{x}}, \theta_k^{\mathrm{y}})$ is referred to as the physical angle pair of UT k. Considering the long distance between satellite and UT k, $\mathbf{g}_k$ changes quite slowly, and we assume that it can be perfectly known at the satellite. The space angle pair $\tilde{\boldsymbol{\theta}}_k = (\tilde{\theta}_k^{\mathrm{x}}, \tilde{\theta}_k^{\mathrm{y}})$ of UT k is defined as $\tilde{\theta}_k^{\mathrm{x}} = \sin\theta_k^{\mathrm{y}} \cos\theta_k^{\mathrm{x}} \in [-1, 1]$ and $\tilde{\theta}_k^{\mathrm{y}} = \cos\theta_k^{\mathrm{y}} \in [-1, 1]$, which reflects the space domain property of UT k's channel [37]. In addition, the physical angle pair $\boldsymbol{\theta}_k$ and nadir angle ϑ_k of UT k depicted in Fig. 1 are related as $\cos\vartheta_k = \sin\theta_k^{\mathrm{y}} \sin\theta_k^{\mathrm{x}}$.

To alleviate the influence of large Doppler shifts and propagation delays in LEO satellite channel, we will perform Doppler and delay compensation for the received signals at each UT in Section II-C.

C. DL Signal Model With Doppler and Delay Compensation

We consider a wideband orthogonal frequency division multiplex (OFDM) satellite system. The number of subcarriers is N_{sc}, and the cyclic prefix (CP) length is N_{cp}. Let T_{s} be the system sampling period. The CP length of time is $T_{\mathrm{cp}} = N_{\mathrm{cp}} T_{\mathrm{s}}$. The OFDM symbol without and with CP are spanned by $T_{\mathrm{sc}} = N_{\mathrm{sc}} T_{\mathrm{s}}$ and $T = T_{\mathrm{sc}} + T_{\mathrm{cp}}$, respectively.

Let $\{\mathbf{x}_{s,r}\}_{r=0}^{N_{\mathrm{sc}}-1}$ be the DL frequency domain transmit signal within the sth OFDM symbol. Then the associated DL time domain transmit signal at OFDM symbol s is given by [40]

$$\mathbf{x}_s(t) = \sum_{r=0}^{N_{\mathrm{sc}}-1} \mathbf{x}_{s,r} e^{j2\pi r \Delta f \cdot t}, \ -T_{\mathrm{cp}} \le t - sT < T_{\mathrm{sc}}, \tag{2}$$

where $\Delta f = 1/T_{\mathrm{sc}}$. By omitting the additive noise temporarily for simplicity, the DL time domain received signal of UT k at OFDM symbol s can be written as

$$\mathbf{y}_{k,s}(t) = \int_{\tau_k^{\min}}^{\tau_k^{\max}} \check{\mathbf{H}}_k(t, \tau) \mathbf{x}_s(t - \tau) \mathrm{d}\tau, \tag{3}$$

where $\check{\mathbf{H}}_k(t, \tau) = \sum_{\ell=0}^{L_k-1} a_{k,\ell} e^{j2\pi\nu_{k,\ell} t} \delta\left(\tau - \tau_{k,\ell}\right) \mathbf{d}_{k,\ell} \cdot \mathbf{g}_k^H$ is the DL channel impulse response of UT k. By exploiting the LEO satellite channel characteristics, we preform the joint Doppler and delay compensation at each UT. Let $\nu_k^{\mathrm{cps}} = \nu_k^{\mathrm{sat}}$ and $\tau_k^{\mathrm{cps}} = \tau_k^{\min}$. Inspired by [37], the compensated DL received signal of UT k is given by

$$\mathbf{y}_{k,s}^{\mathrm{cps}}(t) = \mathbf{y}_{k,s}(t + \tau_k^{\mathrm{cps}}) e^{-j2\pi\nu_k^{\mathrm{cps}}(t + \tau_k^{\mathrm{cps}})}. \tag{4}$$

After Doppler and delay compensation, we choose appropriate OFDM parameters to combat multipath fading effect. The frequency representation of $\mathbf{y}_{k,s}^{\mathrm{cps}}(t)$ can be written as [40]

$$\mathbf{y}_{k,s}^{\mathrm{cps}}(t) = \sum_{r=0}^{N_{\mathrm{sc}}-1} \mathbf{y}_{k,s,r} e^{j2\pi r \Delta f \cdot t}, \ -T_{\mathrm{cp}} + \Delta\tau_k \le t - sT < T_{\mathrm{sc}}, \tag{5}$$

where $\Delta\tau_k = \tau_k^{\max} - \tau_k^{\min}$ is the delay span of UT k's channel [40]. Let $\tau_{k,\ell}^{\mathrm{ut}} = \tau_{k,\ell} - \tau_k^{\min}$, and define the effective DL channel matrix $\mathbf{H}_k(t,f)$ after Doppler and delay compensation as

$$\mathbf{H}_k(t,f) = \mathbf{d}_k(t,f) \cdot \mathbf{g}_k^H, \tag{6}$$

where $\mathbf{d}_k(t,f) = \sum_{\ell=0}^{L_k-1} a_{k,\ell} e^{j2\pi\left(\nu_{k,\ell}^{\mathrm{ut}} t - f\tau_{k,\ell}^{\mathrm{ut}}\right)} \mathbf{d}_{k,\ell} \in \mathbb{C}^{N\times 1}$. Consequently, the DL compensated received signal of UT k over subcarrier r in OFDM symbol s is given by $\mathbf{y}_{k,s,r} = \mathbf{H}_{k,s,r}\mathbf{x}_{s,r}$, where $\mathbf{H}_{k,s,r} = \mathbf{H}_k\left(sT, r\Delta f\right) = \mathbf{d}_k\left(sT, r\Delta f\right)\mathbf{g}_k^H = \mathbf{d}_{k,s,r}\mathbf{g}_k^H$ is the effective DL channel matrix of UT k over subcarrier r in OFDM symbol s after compensation. Since the Doppler and delay have been compensated at each UT, the time and frequency at the satellite and UTs are assumed to be perfectly synchronized in the following.

III. DL Transmit Design

In this section, we investigate the DL transmit design for massive MIMO LEO SATCOM based on the established LEO satellite channel model in Section II. First, by exploiting the LEO satellite channel characteristics, we show that the rank of DL transmit covariance matrix of each UT must be no larger than one to maximize the ergodic sum rate, which indicates that the DL precoding with at most one single data stream for each UT can achieve the optimal performance for linear transmitters, even if each UT has multiple antennas. The optimal DL linear receivers are also obtained as the by-product for single data stream transmission to each UT. After that, we resort to the MM algorithm to obtain a locally optimal solution to the DL precoder design.

A. Rank-One Property of DL Transmit Covariance Matrices

We consider the DL transmission phase in LEO SATCOM where K UTs are simultaneously served on subcarrier r of OFDM symbol s. For convenience, we omit the subscript of OFDM symbol s and subcarrier r in $\mathbf{H}_{k,s,r} = \mathbf{d}_{k,s,r}\mathbf{g}_k$ and denote $\mathbf{H}_k = \mathbf{d}_k\mathbf{g}_k^H$ as the DL channel matrix of UT k. In this paper, the channel $\mathbf{H}_k$ is supposed to be Rician distributed as follows

$$\mathbf{H}_k = \mathbf{d}_k\mathbf{g}_k^H = \sqrt{\frac{\kappa_k\beta_k}{\kappa_k+1}}\bar{\mathbf{H}}_k + \sqrt{\frac{\beta_k}{\kappa_k+1}}\tilde{\mathbf{H}}_k, \tag{7}$$

where $\beta_k = \mathbb{E}\left\{\|\mathbf{H}_k\|_{\mathrm{F}}^2\right\} = \mathbb{E}\left\{\|\mathbf{d}_k\|^2\right\}$ is the average channel power, κ_k is the Rician factor, $\bar{\mathbf{H}}_k = \mathbf{d}_{k,0}\mathbf{g}_k^H$ is the deterministic line-of-sight (LoS) part, $\tilde{\mathbf{H}}_k = \tilde{\mathbf{d}}_k\mathbf{g}_k^H$ is the random scattering part. Besides, $\tilde{\mathbf{d}}_k$ is distributed as $\tilde{\mathbf{d}}_k \sim \mathcal{CN}(\mathbf{0}, \mathbf{\Sigma}_k)$ with $\mathrm{tr}(\mathbf{\Sigma}_k) = 1$. The channel parameters $\mathcal{H} \triangleq \{\beta_k, \kappa_k, \mathbf{g}_k, \mathbf{d}_{k,0}, \mathbf{\Sigma}_k\}_{k=1}^K$ should adapt to the operating frequency bands and the channel conditions [15]. We also suppose that the satellite and UTs move within a certain range, such

that the channel parameters $\mathcal{H}$ can be considered as nearly unchanged. Whenever the satellite or some UT steps out of this range, the channel parameters $\mathcal{H}$ should be updated accordingly. The channel correlation matrices of UT k at the satellite and UT sides are given by

$$\mathbf{R}_k^{\mathrm{sat}} = \mathbb{E}\left\{\mathbf{H}_k^H \mathbf{H}_k\right\} = \beta_k \mathbf{g}_k \mathbf{g}_k^H, \tag{8a}$$

$$\mathbf{R}_k^{\mathrm{ut}} = \mathbb{E}\left\{\mathbf{H}_k \mathbf{H}_k^H\right\} = \frac{\kappa_k \beta_k}{\kappa_k + 1} \mathbf{d}_{k,0} \mathbf{d}_{k,0}^H + \frac{\beta_k}{\kappa_k + 1} \mathbf{\Sigma}_k, \tag{8b}$$

respectively. The matrix $\mathbf{R}_k^{\mathrm{sat}}$ is rank-one, which implies that the signals on different antennas at the satellite are highly correlated. Meanwhile, the rank of matrix $\mathbf{R}_k^{\mathrm{ut}}$ depends on the specific propagation environment around UT k. Denote the UT index set as $\mathcal{K} = \{1, \ldots, K\}$. The DL received signal of UT k is given by

$$\mathbf{y}_k = \mathbf{H}_k \sum_{i=1}^{K} \mathbf{s}_i + \mathbf{z}_k, \tag{9}$$

where $\mathbf{s}_k \in \mathbb{C}^{M \times 1}$ is the desired signal of UT k with zero mean and covariance matrix $\mathbf{Q}_k = \mathbb{E}\{\mathbf{s}_k \mathbf{s}_k^H\}$. In this paper, we consider the sum power constraint $\sum_{k=1}^{K} \mathrm{tr}(\mathbf{Q}_k) \leq P$ for DL transmission. Besides, $\mathbf{z}_k \in \mathbb{C}^{N \times 1}$ is the additive complex Gaussian noise at UT k distributed as $\mathbf{z}_k \sim \mathcal{CN}\left(0, \sigma_k^2 \mathbf{I}_N\right)$. The DL ergodic rate of UT k is defined as

$$\begin{aligned} \mathcal{I}_k &= \mathbb{E}\left\{\log_2 \frac{\det\left(\sigma_k^2 \mathbf{I}_N + \mathbf{H}_k \sum_{i=1}^{K} \mathbf{Q}_i \mathbf{H}_k^H\right)}{\det\left(\sigma_k^2 \mathbf{I}_N + \mathbf{H}_k \sum_{i \neq k} \mathbf{Q}_i \mathbf{H}_k^H\right)}\right\} \\ &\overset{\text{(a)}}{=} \mathbb{E}\left\{\log_2\left(1 + \frac{\mathbf{g}_k^H \mathbf{Q}_k \mathbf{g}_k \|\mathbf{d}_k\|^2}{\sum_{i \neq k} \mathbf{g}_k^H \mathbf{Q}_i \mathbf{g}_k \|\mathbf{d}_k\|^2 + \sigma_k^2}\right)\right\}, \end{aligned} \tag{10}$$

where (a) follows from $\det(\mathbf{I} + \mathbf{AB}) = \det(\mathbf{I} + \mathbf{BA})$ [41]. The DL sum rate maximization problem can be formulated as

$$\mathcal{P}: \max_{\{\mathbf{Q}_k\}_{k=1}^K} \sum_{k=1}^{K} \mathcal{I}_k, \ \text{s.t.} \ \sum_{k=1}^{K} \mathrm{tr}(\mathbf{Q}_k) \leq P, \ \mathbf{Q}_k \succeq \mathbf{0}, \ \forall k \in \mathcal{K}. \tag{11}$$

Proposition 1: The optimal $\{\mathbf{Q}_k\}_{k=1}^K$ to the problem $\mathcal{P}$ must satisfy $\mathrm{rank}(\mathbf{Q}_k) \leq 1$, $\forall k \in \mathcal{K}$.

Proof: Please refer to Appendix A. ■

In Proposition 1, we show that the rank of optimal transmit covariance matrix of each UT should be no larger than one, which indicates that the DL precoding with at most one data stream for each UT is optimal for linear transmitters even though each UT has multiple antennas. This rank property in Proposition 1 results from the massive MIMO LEO satellite channel property. Consequently, we can always write the optimal $\mathbf{Q}_k$ as $\mathbf{Q}_k = \mathbf{w}_k \mathbf{w}_k^H$, where $\mathbf{w}_k \in \mathbb{C}^{M \times 1}$ is the

precoding vector of UT k. Substituting $\mathbf{Q}_k = \mathbf{w}_k \mathbf{w}_k^H$ into (10) yields

$$\mathcal{R}_k = \mathbb{E}\left\{ \log_2 \left(1 + \frac{\left|\mathbf{w}_k^H \mathbf{g}_k\right|^2 \|\mathbf{d}_k\|^2}{\sum_{i \neq k} \left|\mathbf{w}_i^H \mathbf{g}_k\right|^2 \|\mathbf{d}_k\|^2 + \sigma_k^2} \right) \right\}, \tag{12}$$

which is the DL ergodic rate of UT k by using linear precoders $\{\mathbf{w}_k\}_{k=1}^K$. Although we focus on the DL transmit design in this paper, the optimal DL linear receivers at the UT sides are also obtained as the by-product. In the following subsection, we will account for the optimal DL linear receivers of each UT that can maximize their corresponding DL ergodic rates.

B. Optimal DL Linear Receiver

According to Proposition 1, the satellite only needs to send at most one data stream to each UT. Hence, each UT just needs to decode at most one data stream, and only diversity gain is obtained with multiple antennas at UT side. When we use $\{\mathbf{w}_k\}_{k=1}^K$ as the DL linear precoders, the transmit signal $\mathbf{s}_k$ in (9) can be written as $\mathbf{s}_k = \mathbf{w}_k s_k$ where s_k is the intended data symbol for UT k with zero mean and unit variance. We consider that UT k adopts a liner receiver $\mathbf{c}_k \in \mathbb{C}^{N \times 1}$ to recover s_k. Then, the recovered data symbol at UT k can be written as

$$\hat{s}_k = \mathbf{c}_k^H \mathbf{y}_k = \mathbf{c}_k^H \mathbf{d}_k \mathbf{g}_k^H \mathbf{w}_k s_k + \sum_{i \neq k}^{K} \mathbf{c}_k^H \mathbf{d}_k \mathbf{g}_k^H \mathbf{w}_i s_i + \mathbf{c}_k^H \mathbf{z}_k. \tag{13}$$

Thus, the DL signal-to-interference-plus-noise ratio (SINR) of UT k can be expressed as

$$\mathrm{SINR}_k = \frac{\left|\mathbf{w}_k^H \mathbf{g}_k\right|^2 \left|\mathbf{c}_k^H \mathbf{d}_k\right|^2}{\sum_{i \neq k} \left|\mathbf{w}_i^H \mathbf{g}_k\right|^2 \left|\mathbf{c}_k^H \mathbf{d}_k\right|^2 + \sigma_k^2 \left\|\mathbf{c}_k\right\|^2}. \tag{14}$$

Because $\frac{ax}{bx+c}$ is a monotonically increasing function of x for $a, b, c > 0$, we have

$$\mathrm{SINR}_k \overset{\text{(a)}}{\leq} \frac{\left|\mathbf{w}_k^H \mathbf{g}_k\right|^2 \|\mathbf{d}_k\|^2}{\sum_{i \neq k} \left|\mathbf{w}_i^H \mathbf{g}_k\right|^2 \|\mathbf{d}_k\|^2 + \sigma_k^2} \triangleq \underline{\mathrm{SINR}}_k, \tag{15}$$

where (a) follows from the Cauchy-Schwarz inequality $|\mathbf{c}_k^H \mathbf{d}_k|^2 \leq \|\mathbf{c}_k\|^2 \|\mathbf{d}_k\|^2$, and the equality holds if and only if $\mathbf{c}_k = \alpha \mathbf{d}_k$ for any nonzero $\alpha \in \mathbb{C}$. The receivers satisfying $\mathbf{c}_k = \alpha \mathbf{d}_k$ for different α will have the same value of SINR_k. It is worth noting that $\mathbf{c}_k = \alpha \mathbf{d}_k$ can actually maximize the DL ergodic rate of UT k. This can be easily verified by $\mathbb{E}\left\{\log_2(1 + \mathrm{SINR}_k)\right\} \leq \mathbb{E}\left\{\log_2(1 + \underline{\mathrm{SINR}}_k)\right\} = \mathcal{R}_k$, which implies that the receivers satisfying $\mathbf{c}_k = \alpha \mathbf{d}_k$ will be optimal for UT k. Two examples of $\mathbf{c}_k$ with the form $\mathbf{c}_k = \alpha \mathbf{d}_k$ will be given in the following.

One is the receiver $\mathbf{c}_k^{\mathrm{ut}} \triangleq \mathbf{d}_k$, which can be regarded as the matched filter (MF) for the equivalent channel vector $\mathbf{d}_k$, because $\mathbf{y}_k$ can be rewritten as

$$\mathbf{y}_k = \mathbf{d}_k \cdot x_k + \mathbf{z}_k, \tag{16}$$

where $x_k = \sum_{i=1}^K \mathbf{g}_k^H \mathbf{w}_i s_i$ consists of the desired transmit signal and interference for UT k.

The other is the minimum mean-square error (MMSE) receiver [42]

$$\mathbf{c}_k^{\mathrm{mmse}} = \arg\min_{\mathbf{c}_k} \mathrm{MSE}_k \overset{\text{(a)}}{=} \frac{\mathbf{g}_k^H \mathbf{w}_k}{\sigma_k^2 + \sum_{i=1}^K \left|\mathbf{w}_i^H \mathbf{g}_k\right|^2 \|\mathbf{d}_k\|^2} \cdot \mathbf{d}_k, \tag{17}$$

where MSE_k is the mean-square error (MSE) of UT k defined as

$$\mathrm{MSE}_k = \mathbb{E}\left\{|\hat{s}_k - s_k|^2\right\} = \sum_{i=1}^K \left|\mathbf{w}_i^H \mathbf{g}_k\right|^2 \left|\mathbf{c}_k^H \mathbf{d}_k\right|^2 + \sigma_k^2 \|\mathbf{c}_k\|^2 - 2\Re\left\{\mathbf{g}_k^H \mathbf{w}_k \cdot \mathbf{c}_k^H \mathbf{d}_k\right\} + 1, \tag{18}$$

and (a) follows from the matrix inversion lemma [41]. The MMSE of UT k achieved by $\mathbf{c}_k^{\mathrm{mmse}}$ is given by

$$\mathrm{MMSE}_k = 1 - \frac{\left|\mathbf{w}_k^H \mathbf{g}_k\right|^2 \|\mathbf{d}_k\|^2}{\sigma_k^2 + \sum_{i=1}^K \left|\mathbf{w}_i^H \mathbf{g}_k\right|^2 \|\mathbf{d}_k\|^2} = \frac{1}{1 + \underline{\mathrm{SINR}}_k}. \tag{19}$$

Even though $\mathbf{c}_k^{\mathrm{mmse}}$ is related to $\{\mathbf{w}_k\}_{k=1}^K$ and $\mathbf{g}_k$, the scalar term in $\mathbf{c}_k^{\mathrm{mmse}}$ will not affect the value of SINR_k. For simplicity, we can choose $\mathbf{c}_k^{\mathrm{ut}}$ as the DL receiver of UT k, which is easier to be calculated, and independent of $\{\mathbf{w}_k\}_{k=1}^K$ and $\mathbf{g}_k$. Now, we will return to the DL precoder design in the following subsection.

C. DL Precoder Design

In this subsection, we study the DL precoder design by maximizing ergodic sum rate under sum power constraint. Considering that the DL precoder design is a non-convex program, we adopt the MM algorithm [43] combined with the Monte-Carlo method to solve it. In each iteration of MM algorithm, a concave lower bound of the objective function is constructed, and a locally optimal solution can be obtained by solving the convex subproblems iteratively [43].

Let $\mathbf{W} = [\mathbf{w}_1 \ \ldots \ \mathbf{w}_K] \in \mathbb{C}^{M \times K}$ denote the collection of DL precoding vectors. The DL precoder design can be formulated as

$$\mathcal{S}: \ \max_{\mathbf{W}} \ \sum_{k=1}^K \mathcal{R}_k, \quad \text{s.t.} \ \sum_{k=1}^K \|\mathbf{w}_k\|^2 \leq P. \tag{20}$$

Notice that the power inequality in (20) must be met with equality at the optimum. Otherwise, $\mathbf{w}_k$ can be scaled up, which increases the DL sum rate and contradicts the optimality.

In the following, we apply the MM algorithm to calculate a locally optimal solution to $\mathcal{S}$. In each iteration, the DL ergodic rate $\mathcal{R}_k$ is replaced with its concave minorizing function. Then a locally optimal solution to $\mathcal{S}$ can be obtained by solving a sequence of convex programs iteratively. By making use of the relationship between ergodic rate and MMSE [36], for given precoders $\mathbf{W}^{(n)}$ in the nth iteration, we can construct a minorizing function of $\mathcal{R}_k$ as follows

$$g_k^{(n)} = -\frac{1}{\ln 2} \cdot \left(a_k^{(n)} \sum_{i=1}^K \left|\mathbf{w}_i^H \mathbf{g}_k\right|^2 - 2\Re\left\{\mathbf{w}_k^H \mathbf{g}_k \cdot b_k^{(n)}\right\} + c_k^{(n)} \right) + \frac{1}{\ln 2} + \mathcal{R}_k^{(n)}, \tag{21}$$

Algorithm 1 Precoder design algorithm for solving $\mathcal{S}$.

Input: Initialize precoders $\mathbf{w}_k^{(0)} = \mathbf{w}_k^{\text{init}}$ for any $k \in \mathcal{K}$, and iteration index $n = 0$.
Output: Locally optimal precoders $\mathbf{W}$.
1: **while** 1 **do**
2: Calculate $a_k^{(n)}$ and $b_k^{(n)}$ for all $k \in \mathcal{K}$.
3: Update precoders according to (24).
4: **if** $\left| \sum_{k=1}^{K} \mathcal{R}_k^{(n+1)} - \sum_{k=1}^{K} \mathcal{R}_k^{(n)} \right| < \epsilon$, **break**; **else** set $n := n + 1$.
5: **end while**

where $a_k^{(n)}$, $b_k^{(n)}$ and $c_k^{(n)}$ are constants defined in Appendix B. By using the minorizing function $g_k^{(n)}$ in (21), the precoders $\mathbf{W}^{(n+1)}$ in the $(n+1)$th iteration can be obtained by solving the following convex program

$$\mathcal{S}^{(n)}: \max_{\mathbf{W}} \sum_{k=1}^{K} g_k^{(n)}, \quad \text{s.t.} \sum_{k=1}^{K} \|\mathbf{w}_k\|^2 \leq P, \tag{22}$$

which is equivalent to

$$\mathcal{S}^{(n)}: \min_{\mathbf{W}} \sum_{k=1}^{K} \left(\sum_{i=1}^{K} a_i^{(n)} \left| \mathbf{w}_k^H \mathbf{g}_i \right|^2 - 2\Re \left\{ \mathbf{w}_k^H \mathbf{g}_k \cdot b_k^{(n)} \right\} \right), \quad \text{s.t.} \sum_{k=1}^{K} \|\mathbf{w}_k\|^2 \leq P. \tag{23}$$

The optimal solution to $\mathcal{S}^{(n)}$ can be derived easily by using Lagrangian minimization in convex optimizations. Thus, the precoders $\mathbf{W}^{(n+1)}$ are given by

$$\mathbf{w}_k^{(n+1)} = \left(\sum_{i=1}^{K} a_i^{(n)} \mathbf{g}_i \mathbf{g}_i^H + \mu^{(n)} \mathbf{I}_M \right)^{-1} \mathbf{g}_k \cdot b_k^{(n)}, \forall k \in \mathcal{K}, \tag{24}$$

where $\mu^{(n)} \geq 0$ is chosen to make $\sum_{k=1}^{K} \|\mathbf{w}_k^{(n+1)}\|^2 = P$. The DL precoder design algorithm is summarized in Algorithm 1.

Due to the mathematical expectation in the ergodic rate $\mathcal{R}_k$, Monte-Carlo method is required to compute precoders in each iteration of Algorithm 1, which takes plenty of time on exhaustive sample average. In the next section, we will present the low-complexity simplified DL transmit design to avoid the sample average.

IV. Simplified DL Transmit Design

In Section III, Monte-Carlo method with sample average is used to solve the DL precoder design, which is a very time consuming process. To reduce the computation complexity in Monte-Carlo method, we simplify the DL transmit design by using an upper bound of the ergodic sum rate in this section. We show that the DL transmit covariance matrices with rank no large than

one are also optimal, and the corresponding simplified DL precoder design is formulated in terms of the upper bound. Then, we derive the structure of DL precoders and formulate the LMO problem. Finally, a low-complexity algorithm is proposed to solve the LMO problem.

A. Simplified DL Precoder Design

Because $f(x)=\log_2\left(1+\frac{ax}{bx+c}\right)$ is a concave function of $x\geq 0$ for $a,b,c\geq 0$, by invoking the Jensen's inequality [44], the DL ergodic rate $\mathcal{R}_k$ of UT k can be upper bounded by

$$\begin{aligned}\mathcal{I}_k&=\mathbb{E}\left\{\log_2\left(1+\frac{\mathbf{g}_k^H\mathbf{Q}_k\mathbf{g}_k\|\mathbf{d}_k\|^2}{\sum_{i\neq k}\mathbf{g}_k^H\mathbf{Q}_i\mathbf{g}_k\|\mathbf{d}_k\|^2+\sigma_k^2}\right)\right\}\\&\leq\log_2\left(1+\frac{\mathbf{g}_k^H\mathbf{Q}_k\mathbf{g}_k\beta_k}{\sum_{i\neq k}\mathbf{g}_k^H\mathbf{Q}_i\mathbf{g}_k\beta_k+\sigma_k^2}\right)\triangleq\mathcal{I}_k^{\mathrm{ub}}.\end{aligned}\tag{25}$$

The problem of maximizing the upper bound of DL ergodic sum rate can be formulated as

$$\mathcal{P}^{\mathrm{ub}}:\ \max_{\{\mathbf{Q}_k\}_{k=1}^K}\sum_{k=1}^K\mathcal{I}_k^{\mathrm{ub}},\ \text{s.t.}\ \sum_{k=1}^K\mathrm{tr}(\mathbf{Q}_k)\leq P,\ \mathbf{Q}_k\succeq\mathbf{0},\ \forall k\in\mathcal{K}.\tag{26}$$

Corollary 1: The optimal $\{\mathbf{Q}_k\}_{k=1}^K$ to the problem $\mathcal{P}^{\mathrm{ub}}$ must satisfy $\mathrm{rank}(\mathbf{Q}_k)\leq 1,\ \forall k\in\mathcal{K}$.

Proof: The proof is similar with that in Proposition 1. Thus, it is omitted here. ■

According to Corollary 1, the transmit covariance matrices with rank no larger than one are also sufficient to maximize the upper bound of DL ergodic sum rate. Thus, we can rewrite the transmit covariance matrix $\mathbf{Q}_k$ as $\mathbf{Q}_k=\mathbf{w}_k\mathbf{w}_k^H$, and the upper bound of $\mathcal{R}_k$ is given by

$$\mathcal{R}_k\leq\log_2\left(1+\frac{\left|\mathbf{w}_k^H\mathbf{g}_k\right|^2\beta_k}{\sum_{i\neq k}\left|\mathbf{w}_i^H\mathbf{g}_k\right|^2\beta_k+\sigma_k^2}\right)\triangleq\mathcal{R}_k^{\mathrm{ub}}.\tag{27}$$

The simplified DL precoder design by using the upper bound $\mathcal{R}_k^{\mathrm{ub}}$ can be formulated as

$$\mathcal{S}^{\mathrm{ub}}:\ \max_{\mathbf{W}}\ \sum_{k=1}^K\mathcal{R}_k^{\mathrm{ub}},\quad\text{s.t.}\ \sum_{k=1}^K\|\mathbf{w}_k\|^2\leq P.\tag{28}$$

Notice that in the simplified precoder design $\mathcal{S}^{\mathrm{ub}}$, only the channel parameters $\{\beta_k,\mathbf{g}_k\}_{k=1}^K$ are required at the satellite to compute precoding vectors, which can be obtained through the off-the-shelf parameter estimation techniques [42], [45]. The iteratively weighted MMSE (WMMSE) approach can be used to solve $\mathcal{S}^{\mathrm{ub}}$, which guarantees convergence to a locally optimal solution of $\mathcal{S}^{\mathrm{ub}}$ [46]. The detailed description of WMMSE algorithm can be found in [46]. Here, for simplicity, we only give the updating formulas of DL precoders

$$\mathbf{w}_k^{(n+1)}=\left(\sum_{i=1}^K\tilde{a}_i^{(n)}\mathbf{g}_i\mathbf{g}_i^H+\tilde{\mu}^{(n)}\mathbf{I}_M\right)^{-1}\mathbf{g}_k\cdot\tilde{b}_k^{(n)},\ \forall k\in\mathcal{K},\tag{29}$$

Algorithm 2 Simplified precoder design algorithm for solving $\mathcal{S}^{\mathrm{ub}}$.

Input: Initialize precoders $\mathbf{w}_k^{(0)} = \mathbf{w}_k^{\mathrm{init}}$ for any $k \in \mathcal{K}$, and iteration index $n = 0$.
Output: Locally optimal precoder $\mathbf{W}$.
1: **while** 1 **do**
2: Calculate $\tilde{a}_k^{(n)}$ and $\tilde{b}_k^{(n)}$ for all $k \in \mathcal{K}$.
3: Update precoders according to (29).
4: **if** $\left| \sum_{k=1}^{K} \mathcal{R}_k^{(n+1)} - \sum_{k=1}^{K} \mathcal{R}_k^{(n)} \right| < \epsilon$, **break**; **else** set $n := n + 1$.
5: **end while**

where $\tilde{a}_k^{(n)} = \frac{\beta_k}{\sigma_k^2 + \sum_{i \neq k} |\mathbf{g}_k^H \mathbf{w}_i^{(n)}|^2 \beta_k} - \frac{\beta_k}{\sigma_k^2 + \sum_{i=1}^{K} |\mathbf{g}_k^H \mathbf{w}_i^{(n)}|^2 \beta_k}$ and $\tilde{b}_k^{(n)} = \frac{\beta_k \cdot \mathbf{g}_k^H \mathbf{w}_k^{(n)}}{\sigma_k^2 + \sum_{i \neq k} |\mathbf{g}_k^H \mathbf{w}_i^{(n)}|^2 \beta_k}$. The dual variable $\tilde{\mu}^{(n)} \geq 0$ in (29) can be obtained by bisection search to make $\sum_{k=1}^{K} \|\mathbf{w}_k^{(n+1)}\|^2 = P$. The complete WMMSE algorithm is summarized in Algorithm 2.

Algorithm 2 consists of outer and inner iterations. In each outer iteration, the precoding vectors are updated according to (29). In the inner iteration, multiplying the inverse of an M-dimensional matrix with K vectors are performed to obtain the optimal $\tilde{\mu}^{(n)}$ with bisection search. The complexity of Algorithm 2 is mainly evaluated by the multiplication number in matrix operations given by $N_{\mathrm{out}} N_{\mathrm{in}} (M^3 + KM^2)$, where N_{out} and N_{in} are numbers of outer and inner iterations, respectively.

B. Structure of DL Precoder

In this subsection, we aim to study the structure of optimal DL precoders for $\mathcal{S}^{\mathrm{ub}}$. First, we formulate a quality of service (QoS) problem with properly chosen thresholds, which has the same optimal solution with $\mathcal{S}^{\mathrm{ub}}$ and is easier to be solved. Then, the structure of optimal solution to $\mathcal{S}^{\mathrm{ub}}$ can be fully characterized by that to the QoS problem. Based on the structure, the simplified DL precoder design $\mathcal{S}^{\mathrm{ub}}$ can be converted into an LMO problem, where there is only one scalar to be optimized for each UT.

Let r_k be the optimal $\mathcal{R}_k^{\mathrm{ub}}$ in $\mathcal{S}^{\mathrm{ub}}$. We can formulate a QoS problem as follows

$$\mathcal{Q}^{\mathrm{ub}}: \min_{\mathbf{W}} \sum_{k=1}^{K} \|\mathbf{w}_k\|^2, \text{ s.t. } \mathcal{R}_k^{\mathrm{ub}} \geq r_k, \forall k \in \mathcal{K}, \tag{30}$$

where r_k is the rate threshold of UT k. Now, the problems $\mathcal{Q}^{\mathrm{ub}}$ and $\mathcal{S}^{\mathrm{ub}}$ will have the same optimal solution, and the optimal value of $\mathcal{Q}^{\mathrm{ub}}$ is P [47]. The explanations will be stated in the following. Notice that the optimal solution to $\mathcal{S}^{\mathrm{ub}}$ must be feasible to $\mathcal{Q}^{\mathrm{ub}}$. If $\mathcal{Q}^{\mathrm{ub}}$ has the optimal value which is less than P, then we can always scale up the optimal solution to $\mathcal{Q}^{\mathrm{ub}}$ such

that $\mathcal{R}_k^{\rm ub} > r_k$ and the power constraint in $\mathcal{S}^{\rm ub}$ is still fulfilled, which contradicts the optimality of r_k. Hence, we can learn the structure of optimal solution to $\mathcal{S}^{\rm ub}$ by studying that to $\mathcal{Q}^{\rm ub}$. Denote $\gamma_k = 2^{r_k} - 1$. The problem $\mathcal{Q}^{\rm ub}$ can be reformulated as

$$\mathcal{Q}^{\rm ub}: \min_{\mathbf{W}} \sum_{k=1}^{K} \|\mathbf{w}_k\|^2, \text{ s.t. } \frac{\beta_k}{\gamma_k \sigma_k^2} \left|\mathbf{w}_k^H \mathbf{g}_k\right|^2 \geq \frac{\beta_k}{\sigma_k^2} \sum_{i \neq k} \left|\mathbf{w}_i^H \mathbf{g}_k\right|^2 + 1, \, \forall k \in \mathcal{K}, \tag{31}$$

which is actually a quadratically constrained quadratic programming (QCQP) [44]. However, the quadratic constraints in (31) are still non-convex. Notice that $e^{j\theta_k}\mathbf{w}_k$ and $\mathbf{w}_k$ can attain the same objective value in $\mathcal{Q}^{\rm ub}$, and they also have the same feasibility for any $\theta_k \in \mathbb{R}$. Therefore, we can always rotate the phase of $\mathbf{w}_k$ to guarantee $\mathbf{w}_k^H \mathbf{g}_k$ is real. Thus, the constraints in (31) can be converted into convex second-order cone (SOC) constraints [47]

$$\sqrt{\frac{\beta_k}{\gamma_k \sigma_k^2}} \Re\left\{\mathbf{w}_k^H \mathbf{g}_k\right\} \geq \sqrt{\frac{\beta_k}{\sigma_k^2} \sum_{i \neq k} \left|\mathbf{w}_i^H \mathbf{g}_k\right|^2 + 1}, \, \forall k \in \mathcal{K}. \tag{32}$$

It is easy to show that the Slater's constraint qualification is satisfied for $\mathcal{Q}^{\rm ub}$ [47]. If the parameters $\{r_k\}_{k=1}^K$ are given, the problem $\mathcal{Q}^{\rm ub}$ can be optimally solved through fixed-point iteration (FPI) or standard SOC programming (SOCP) algorithms [48]. Next, the structure of the optimal solution to $\mathcal{S}^{\rm ub}$ is stated in the following proposition.

Proposition 2: The optimal solution to $\mathcal{S}^{\rm ub}$ satisfies

$$\left(\sum_{i=1}^{K} \frac{\lambda_i \beta_i}{\sigma_i^2} \mathbf{g}_i \mathbf{g}_i^H + \mathbf{I}_M\right)^{-1} \frac{\lambda_k \beta_k}{\sigma_k^2} \mathbf{g}_k \mathbf{g}_k^H \mathbf{w}_k = \frac{\gamma_k}{\gamma_k + 1} \mathbf{w}_k, \tag{33}$$

where $\lambda_k \geq 0$ is the optimal Lagrange multiplier of (31), and satisfies $\sum_{k=1}^K \lambda_k = P$.

Proof: Please refer to Appendix C. ■

It is worth noting that the rate threshold r_k in $\mathcal{Q}^{\rm ub}$ is the optimal $\mathcal{R}_k^{\rm ub}$, which is not available until $\mathcal{S}^{\rm ub}$ is optimally solved. Although the optimal solution to $\mathcal{S}^{\rm ub}$ can be obtained by solving $\mathcal{Q}^{\rm ub}$ for given r_k, the searching of r_k is as difficult as solving $\mathcal{S}^{\rm ub}$ itself. Proposition 2 provides the structure for the optimal solution to $\mathcal{S}^{\rm ub}$, which will facilitate the simplified DL precoder design. From another perspective, if the Lagrange multipliers $\{\lambda_k\}_{k=1}^K$ are given, it can be easily derived from (33) that the normalized precoder $\underline{\mathbf{w}}_k \triangleq \frac{\mathbf{w}_k}{\|\mathbf{w}_k\|}$ and γ_k are given by

$$\underline{\mathbf{w}}_k = \frac{\left(\sum_{i=1}^{K} \frac{\lambda_i \beta_i}{\sigma_i^2} \mathbf{g}_i \mathbf{g}_i^H + \mathbf{I}_M\right)^{-1} \mathbf{g}_k}{\left\|\left(\sum_{i=1}^{K} \frac{\lambda_i \beta_i}{\sigma_i^2} \mathbf{g}_i \mathbf{g}_i^H + \mathbf{I}_M\right)^{-1} \mathbf{g}_k\right\|}, \tag{34}$$

$$\gamma_k = \left(1 - \frac{\lambda_k \beta_k}{\sigma_k^2} \mathbf{g}_k^H \left(\sum_{i=1}^{K} \frac{\lambda_i \beta_i}{\sigma_i^2} \mathbf{g}_i \mathbf{g}_i^H + \mathbf{I}_M \right)^{-1} \mathbf{g}_k \right)^{-1} - 1. \tag{35}$$

Define $\boldsymbol{\lambda} = (\lambda_1, \ldots, \lambda_K)^T$ and $\boldsymbol{\gamma} = (\gamma_1, \ldots, \gamma_K)^T$ as the collection of Lagrange multipliers and thresholds, respectively. If we assume that the Lagrange multipliers $\boldsymbol{\lambda}$ are given, then the normalized precoders $\{\underline{\mathbf{w}}_k\}_{k=1}^K$ and thresholds $\boldsymbol{\gamma}$ can be obtained from (34) and (35), respectively. With the results of $\{\underline{\mathbf{w}}_k\}_{k=1}^K$ and $\boldsymbol{\gamma}$, the power $q_k = \|\mathbf{w}_k\|^2 \, (\forall k \in \mathcal{K})$ can be calculated by [47]

$$\mathbf{q} = \mathbf{M}^{-1} \mathbf{1}, \tag{36}$$

where $\mathbf{q} = (q_1, \ldots, q_K)^T$, and $\mathbf{M} \in \mathbb{R}^{K \times K}$ is defined as

$$[\mathbf{M}]_{k,i} = \begin{cases} -\frac{\beta_k}{\sigma_k^2} \left| \mathbf{g}_k^H \underline{\mathbf{w}}_i \right|^2, & \text{if } k \neq i \\ \frac{\beta_k}{\gamma_k \sigma_k^2} \left| \mathbf{g}_k^H \underline{\mathbf{w}}_k \right|^2, & \text{if } k = i \end{cases}. \tag{37}$$

Then, the precoder $\mathbf{w}_k$ can be calculated by $\mathbf{w}_k = \underline{\mathbf{w}}_k \sqrt{q_k} (\forall k \in \mathcal{K})$, where $\underline{\mathbf{w}}_k$ and q_k are given by (34) and (36), respectively. The relationship between the parameters $\boldsymbol{\lambda}$, $\boldsymbol{\gamma}$ and $\mathbf{W}$ is illustrated in Fig. 2. From Fig. 2, it is shown that if the thresholds $\boldsymbol{\gamma}$ are known, the optimal precoders $\mathbf{W}$ and Lagrange multipliers $\boldsymbol{\lambda}$ can be calculated by solving $\mathcal{Q}^{\text{ub}}$ via FPI or SOCP algorithms. On the other hand, if the Lagrange multipliers $\boldsymbol{\lambda}$ are known, the corresponding precoders $\mathbf{W}$ and thresholds $\boldsymbol{\gamma}$ can be calculated via (34)–(36).

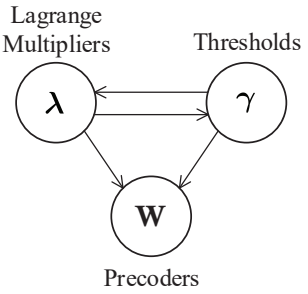

Fig. 2: Relationship between $\boldsymbol{\lambda}$, $\boldsymbol{\gamma}$ and $\mathbf{W}$.

We would like to make more interpretations for the latter case above, before further elaboration of the LMO problem. Now assume that $\boldsymbol{\lambda} \geq \mathbf{0}$ consists of arbitrary Lagrange multipliers with $\sum_{k=1}^K \lambda_k = P$. We can formulate a problem $\mathcal{Q}^{\text{ub}}$ as in (31), where the thresholds $\boldsymbol{\gamma}$ are calculated by (35). Because the duality gap for the problem $\mathcal{Q}^{\text{ub}}$ is zero, the optimal solution to such $\mathcal{Q}^{\text{ub}}$ will satisfy $\sum_{k=1}^K \|\mathbf{w}_k\|^2 = P$. Meanwhile, the optimal Lagrange multipliers of such $\mathcal{Q}^{\text{ub}}$ are equal to $\boldsymbol{\lambda}$ exactly, and the corresponding optimal precoders $\mathbf{W}$ can be calculated by (34) and (36).

C. Low-Complexity DL Precoder Design With LMO

In this subsection, we will convert the problem $\mathcal{S}^{\mathrm{ub}}$ into an LMO problem. Substituting γ_k in (35) into $r_k = \log_2(1+\gamma_k)$ yields

$$\begin{aligned} r_k &= -\log_2\left(1 - \frac{\lambda_k\beta_k}{\sigma_k^2}\mathbf{g}_k^H\left(\sum_{i=1}^{K}\frac{\lambda_i\beta_i}{\sigma_i^2}\mathbf{g}_i\mathbf{g}_i^H + \mathbf{I}_M\right)^{-1}\mathbf{g}_k\right) \\ &\overset{\text{(a)}}{=} \log_2\det\left(\sum_{i=1}^{K}\frac{\lambda_i\beta_i}{\sigma_i^2}\mathbf{g}_i\mathbf{g}_i^H + \mathbf{I}_M\right) - \log_2\det\left(\sum_{i\neq k}\frac{\lambda_i\beta_i}{\sigma_i^2}\mathbf{g}_i\mathbf{g}_i^H + \mathbf{I}_M\right), \end{aligned} \tag{38}$$

where (a) follows from the identity $\det(\mathbf{I}+\mathbf{AB}) = \det(\mathbf{I}+\mathbf{BA})$ [41].

Now, we can formulate an LMO problem as follows

$$\mathcal{M}^{\mathrm{ub}}: \max_{\boldsymbol{\lambda}\geq\mathbf{0}} \sum_{k=1}^{K} r_k, \text{ s.t. } \mathbf{1}^T\boldsymbol{\lambda} = P. \tag{39}$$

In the problem $\mathcal{M}^{\mathrm{ub}}$, there is only one scalar λ_k, rather than a precoding vector $\mathbf{w}_k$, to be optimized for each UT $k \in \mathcal{K}$, which can be exploited in the simplified DL precoder design. The relationship between problems $\mathcal{M}^{\mathrm{ub}}$ and $\mathcal{S}^{\mathrm{ub}}$ are described in the following proposition.

Proposition 3: The problems $\mathcal{M}^{\mathrm{ub}}$ and $\mathcal{S}^{\mathrm{ub}}$ have the same optimal value.

Proof: Please refer to Appendix D. ■

According to Proposition 3, if the problem $\mathcal{M}^{\mathrm{ub}}$ can be optimally solved, then the optimal precoder of $\mathcal{S}^{\mathrm{ub}}$ can be directly obtained via (34) and (36). Hence, the simplified DL precoder design is converted into the LMO problem.

However, since r_k in $\mathcal{M}^{\mathrm{ub}}$ is a non-convex function of $\boldsymbol{\lambda}$, it is still difficult to solve $\mathcal{M}^{\mathrm{ub}}$. Interestingly, we find that r_k is equal to the rate of UT k in a virtual UL multi-user single-input multiple-output (MU-SIMO) channel, and λ_k can be regarded as the virtual UL transmit power of UT k. Finally, we propose a low-complexity algorithm to obtain a locally optimal solution to $\mathcal{M}^{\mathrm{ub}}$.

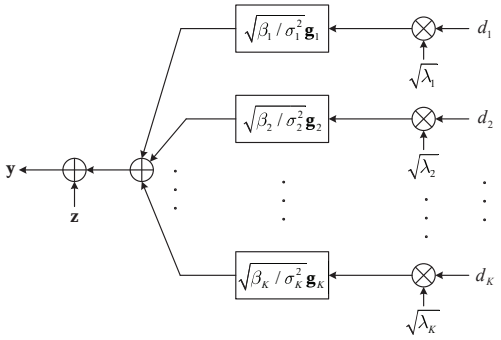

Fig. 3: Virtual UL MU-SIMO channel.

In the virtual UL, each single-antenna UT transmits one data stream to a BS equipped with M antennas. The received signal $\mathbf{y} \in \mathbb{C}^{M\times 1}$ at the BS can be written as

$$\mathbf{y} = \sum_{i=1}^{K} \sqrt{\beta_i/\sigma_i^2}\mathbf{g}_i \cdot \sqrt{\lambda_i} d_i + \mathbf{z}, \tag{40}$$

where $\sqrt{\beta_i/\sigma_i^2}\mathbf{g}_i$ is the channel vector between UT i and the BS, $\lambda_i \geq 0$ and d_i are the transmit power and data symbol of UT i. The data symbol d_i is assumed to have zero mean and unit variance, and $\mathbf{z} \sim \mathcal{CN}(\mathbf{0}, \mathbf{I}_M)$ is the additive complex Gaussian noise. The virtual UL model is shown in Fig. 3.

We assume that the BS decodes the data streams of each UT without successive interference cancellation (SIC) [49]. The BS uses a linear receiver $\mathbf{u}_k \in \mathbb{C}^{M\times 1}$ to recover the data symbol from UT k. Then, the recovered data symbol $\hat{d}_k$ of UT k can be written as

$$\hat{d}_k = \mathbf{u}_k^H \mathbf{y} = \mathbf{u}_k^H \mathbf{g}_k \sqrt{\frac{\lambda_k \beta_k}{\sigma_k^2}} d_k + \sum_{i\neq k} \mathbf{u}_k^H \mathbf{g}_i \sqrt{\frac{\lambda_i \beta_i}{\sigma_i^2}} d_i + \mathbf{u}_k^H \mathbf{z}. \tag{41}$$

The virtual MSE (VMSE) of UT k can be expressed as

$$\mathrm{VMSE}_k = \mathbb{E}\left\{\left|\hat{d}_k - d_k\right|^2\right\} = \sum_{i=1}^{K}\left|\mathbf{u}_k^H \mathbf{g}_i\right|^2 \frac{\lambda_i \beta_i}{\sigma_i^2} - 2\Re\left\{\mathbf{u}_k^H \mathbf{g}_k\right\}\sqrt{\frac{\lambda_k \beta_k}{\sigma_k^2}} + \|\mathbf{u}_k\|^2 + 1. \tag{42}$$

Thus, the $\mathbf{u}_k$ that minimizes VMSE_k is given by

$$\mathbf{u}_k^{\mathrm{vmmse}} = \left(\sum_{i=1}^{K} \frac{\lambda_i \beta_i}{\sigma_i^2}\mathbf{g}_i \mathbf{g}_i^H + \mathbf{I}_M\right)^{-1} \mathbf{g}_k \sqrt{\frac{\lambda_k \beta_k}{\sigma_k^2}}, \tag{43}$$

and the corresponding virtual MMSE (VMMSE) of UT k is

$$\mathrm{VMMSE}_k = 1 - \frac{\lambda_k \beta_k}{\sigma_k^2}\mathbf{g}_k^H \left(\sum_{i=1}^{K} \frac{\lambda_i \beta_i}{\sigma_i^2}\mathbf{g}_i \mathbf{g}_i^H + \mathbf{I}_M\right)^{-1} \mathbf{g}_k. \tag{44}$$

Then, r_k can be rewritten as

$$r_k = -\log_2 \mathrm{VMMSE}_k. \tag{45}$$

Next, we make use of the MM algorithm to obtain a locally optimal solution to $\mathcal{M}^{\mathrm{ub}}$. According to the relationship between r_k and VMMSE_k in (45), a minoring function of r_k is constructed as follows

$$h_k^{(n)} = -\frac{1}{\ln 2}\left(\sum_{i=1}^{K} \psi_{k,i}^{(n)} \frac{\lambda_i \beta_i}{\sigma_i^2} - 2\chi_k^{(n)}\sqrt{\frac{\lambda_k \beta_k}{\sigma_k^2}} + \delta_k^{(n)}\right) + \frac{1}{\ln 2} + r_k^{(n)}, \tag{46}$$

where $\psi_{k,i}^{(n)}$, $\chi_k^{(n)}$ and $\delta_k^{(n)}$ are shown in Appendix E. Then, a locally optimal solution to $\mathcal{M}^{\mathrm{ub}}$

can be obtained by iteratively solving the following convex subproblem

$$\mathcal{M}_n^{\mathrm{ub}}: \max_{\boldsymbol{\lambda}\geq\mathbf{0}} \sum_{k=1}^{K} h_k^{(n)}, \quad \text{s.t. } \mathbf{1}^T\boldsymbol{\lambda} = P, \tag{47}$$

which is equivalent to

$$\mathcal{M}_n^{\mathrm{ub}}: \min_{\boldsymbol{\lambda}\geq\mathbf{0}} \sum_{k=1}^{K}\sum_{i=1}^{K} \psi_{i,k}^{(n)} \frac{\lambda_k\beta_k}{\sigma_k^2} - 2\sum_{k=1}^{K} \chi_k^{(n)} \sqrt{\frac{\lambda_k\beta_k}{\sigma_k^2}}, \quad \text{s.t. } \mathbf{1}^T\boldsymbol{\lambda} = P. \tag{48}$$

By applying the Lagrangian minimization method, the optimal solution to $\mathcal{M}_n^{\mathrm{ub}}$ is given by

$$\sqrt{\lambda_k} = \frac{\chi_k^{(n)}\sqrt{\frac{\beta_k}{\sigma_k^2}}}{\sum_{i=1}^{K}\psi_{i,k}^{(n)}\frac{\beta_k}{\sigma_k^2} + \nu^{(n)}}, \forall k \in \mathcal{K}, \tag{49}$$

where $\nu^{(n)}$ is the dual variable associated with the equality constraint in $\mathcal{M}_n^{\mathrm{ub}}$. To make the right-hand side of (49) non-negative, the dual variable $\nu^{(n)}$ must satisfy $\nu^{(n)} \geq -\min_{k\in\mathcal{K}} \sum_{i=1}^{K} \psi_{i,k}^{(n)} \frac{\beta_k}{\sigma_k^2}$. Hence, the optimal solution to $\mathcal{M}_n^{\mathrm{ub}}$ can be written as

$$\lambda_k^{(n+1)} = \frac{\left(\chi_k^{(n)}\right)^2 \frac{\beta_k}{\sigma_k^2}}{\left(\sum_{i=1}^{K}\psi_{i,k}^{(n)}\frac{\beta_k}{\sigma_k^2} + \nu^{(n)}\right)^2}, \forall k \in \mathcal{K}, \tag{50}$$

where $\nu^{(n)}$ can be obtained by bisection search to make $\sum_{k=1}^{K}\lambda_k^{(n+1)} = P$. The algorithm to solve $\mathcal{M}^{\mathrm{ub}}$ is summarized in Algorithm 3. When the Lagrange multipliers $\boldsymbol{\lambda}$ are calculated with Algorithm 3, the associated DL precoders $\mathbf{W}$ can be determined by (34) and (36).

There are also outer and inner iterations in Algorithm 3. In each outer iteration of Algorithm 3, the M-dimensional matrix inversion and multiplying the inverse matrix with K vectors are conducted to calculate $\psi_{k,i}^{(n)}(\forall k,i \in \mathcal{K})$ and $\chi_k^{(n)}(\forall k \in \mathcal{K})$. Meanwhile, in the inner iterations of Algorithm 3, the computation is performed only for scalar variables. Therefore, the complexity of Algorithm 3 is mainly characterized by $N_{\mathrm{out}}(M^3 + KM^2)$. Compared with Algorithm 2, the complexity of Algorithm 3 is significantly reduced. In addition, the superiority of Algorithm 3 is even more obvious for the case that M or K is extremely large, which makes it quite attractive for massive MIMO LEO SATCOM.

At last, we provide a theoretical analysis for r_k. A lower bound of r_k is given by

$$\begin{aligned} r_k &\overset{\text{(a)}}{=} -\log_2\left[\left(\mathbf{I} + \boldsymbol{\Gamma}^{\frac{1}{2}}\mathbf{G}^H\mathbf{G}\boldsymbol{\Gamma}^{\frac{1}{2}}\right)^{-1}\right]_{k,k} \\ &\overset{\text{(b)}}{=} \log_2\left(1 + \frac{\lambda_k\beta_k}{\sigma_k^2} - \frac{\lambda_k\beta_k}{\sigma_k^2}\mathbf{g}_k^H\underline{\mathbf{G}}_k\underline{\boldsymbol{\Gamma}}_k^{\frac{1}{2}}\left(\mathbf{I} + \underline{\boldsymbol{\Gamma}}_k^{\frac{1}{2}}\underline{\mathbf{G}}_k^H\underline{\mathbf{G}}_k\underline{\boldsymbol{\Gamma}}_k^{\frac{1}{2}}\right)^{-1}\underline{\boldsymbol{\Gamma}}_k^{\frac{1}{2}}\underline{\mathbf{G}}_k^H\mathbf{g}_k\right) \\ &\overset{\text{(c)}}{\geq} \log_2\left(1 + \frac{\lambda_k\beta_k}{\sigma_k^2} - \frac{\lambda_k\beta_k}{\sigma_k^2}\sum_{i\neq k}\frac{\lambda_i\beta_i}{\sigma_i^2}\left|\mathbf{g}_i^H\mathbf{g}_k\right|^2\right), \end{aligned} \tag{51}$$

Algorithm 3 LMO algorithm for solving $\mathcal{M}^{\mathrm{ub}}$.

Input: Initialize Lagrange multipliers $\boldsymbol{\lambda}^{(0)} = \boldsymbol{\lambda}^{\mathrm{init}}$, and iteration index $n = 0$.
Output: Locally optimal Lagrange multipliers $\boldsymbol{\lambda}$ to $\mathcal{M}^{\mathrm{ub}}$.
1: **while** 1 **do**
2: Calculate $\sum_{i=1}^{K} \psi_{i,k}^{(n)}$ and $\chi_k^{(n)}$ for all $k \in \mathcal{K}$.
3: Update Lagrange multipliers according to (50).
4: **if** $\left| \sum_{k=1}^{K} r_k^{(n+1)} - \sum_{k=1}^{K} r_k^{(n)} \right| < \epsilon$, **break**; **else** set $n := n + 1$.
5: **end while**

where $\boldsymbol{\Gamma} = \mathrm{diag}\left(\frac{\lambda_1\beta_1}{\sigma_1^2}, \ldots, \frac{\lambda_K\beta_K}{\sigma_K^2}\right)$, $\mathbf{G} = [\mathbf{g}_1 \ \ldots \ \mathbf{g}_K]$, $\underline{\boldsymbol{\Gamma}}_k$ is the $(K-1)$-dimensional diagonal matrix obtained by deleting the kth diagonal element in $\boldsymbol{\Gamma}$, $\underline{\mathbf{G}}_k$ is an $M \times (K-1)$ matrix obtained by deleting the kth column in $\mathbf{G}$, (a) follows from the matrix inversion lemma [41], (b) follows from the identity in [41, Eq. 0.7.3.1], and (c) follows from the positive semidefinite property of $\underline{\boldsymbol{\Gamma}}_k^{\frac{1}{2}} \underline{\mathbf{G}}_k^H \underline{\mathbf{G}}_k \underline{\boldsymbol{\Gamma}}_k^{\frac{1}{2}}$. From (51), we can see that the multi-user interference is caused by the non-orthogonality between array response vectors $\{\mathbf{g}_k\}_{k=1}^K$.

In addition, an upper bound for the sum of r_k is given by in the following proposition. The necessary and sufficient conditions to achieve the upper bound are also shown.

Proposition 4: The sum of r_k satisfies the following inequality

$$\sum_{k=1}^{K} r_k \leq \sum_{k=1}^{K} \log_2\left(1 + \frac{\lambda_k\beta_k}{\sigma_k^2}\right), \tag{52}$$

and the equality holds if and only if $\mathbf{G}^H\mathbf{G} = \mathbf{I}$.

Proof: Please refer to Appendix F. ■

The condition $\mathbf{G}^H\mathbf{G} = \mathbf{I}$ means that the array response vectors $\{\mathbf{g}_k\}_{k=1}^K$ are orthogonal with each other. Under this condition, the lower bound of r_k in (51) also becomes tight. Then, r_k will reduce to $r_k = \log_2\left(1 + \frac{\lambda_k\beta_k}{\sigma_k^2}\right)$, and the problem $\mathcal{S}^{\mathrm{ub}}$ will reduce to a convex program

$$\max_{\boldsymbol{\lambda} \geq \mathbf{0}} \ \sum_{k=1}^{K} \log_2\left(1 + \frac{\lambda_k\beta_k}{\sigma_k^2}\right), \quad \text{s.t. } \mathbf{1}^T\boldsymbol{\lambda} = P. \tag{53}$$

The optimal $\boldsymbol{\lambda}$ can be calculated by classic water-filling algorithm [49], i.e., $\lambda_k = \left[\frac{1}{\ln 2 \cdot \nu} - \frac{\sigma_k^2}{\beta_k}\right]^+$, $\forall k \in \mathcal{K}$, where $[x]^+ = \max\{x, 0\}$, ν is chosen to make $\mathbf{1}^T\boldsymbol{\lambda} = P$.

V. Simulation Results

In this section, we show the simulation results to verify the performance of the proposed DL transmit designs in massive MIMO LEO SATCOM. The simulation parameters are summarized

TABLE I: Simulation Parameters

Parameters	Values
Earth radius R_e	6378 km
Orbit altitude H	1000 km
Central frequency f_c	2 GHz
Bandwidth B	20 MHz
Noise temperature $T_{\rm n}$	290 K
Number of antennas $M_{\rm x} \times M_{\rm y}$, $N_{\rm x'} \times N_{\rm y'}$	16×16, 6×6
Antenna spacing $d_{\rm x}$, $d_{\rm y}$, $d_{\rm x'}$, $d_{\rm y'}$	λ, λ, $\frac{\lambda}{2}$, $\frac{\lambda}{2}$
Antenna gain $G_{\rm sat}$, $G_{\rm ut}$	3 dB, 0 dB
Multipath number L_k	6
Rician factor κ_k	10 dB
Space angle distribution $\tilde{\theta}_k^{\rm x}$, $\tilde{\theta}_k^{\rm y}$	U $[-0.5, 0.5]$
Number of UTs K	256
Transmit power P	0 dBW – 30 dBW

in TABLE I. As we can see, when the orbit altitude H is fixed, the location distribution of UTs is fully determined by the distribution of their space angle pairs. From TABLE I, the space angle pair $\tilde{\boldsymbol{\theta}}_k = (\tilde{\theta}_k^{\rm x}, \tilde{\theta}_k^{\rm y})$ of UT k is distributed as $\tilde{\theta}_k^{\rm x}$, $\tilde{\theta}_k^{\rm y} \sim$ U $[-0.5, 0.5]$. The antenna spacing at the satellite $d_{\rm x} = d_{\rm y} = \lambda$ is set to avoid grating lobes in the visible interval $[-0.5, 0.5]$ containing $\tilde{\theta}_k^{\rm x}$ and $\tilde{\theta}_k^{\rm y}$ along the x-axis and y-axis, as well as maximize the spatial resolution [50]. The nadir angle ϑ_k of UT k depicted in Fig. 1 is determined from $\vartheta_k = \cos^{-1}\left(\sin\theta_k^{\rm y} \sin\theta_k^{\rm x}\right)$, which satisfies $\vartheta_k \in [0°, 45°]$ because of the relation $\sin\theta_k^{\rm y} \sin\theta_k^{\rm x} = \sqrt{1 - (\tilde{\theta}_k^{\rm y})^2 - (\tilde{\theta}_k^{\rm x})^2}$. Hence, the distance between the satellite and UT k is given by $D_k = \sqrt{R_e^2 + R_s^2 - 2R_eR_s\cos\psi_k}$ [15], where $R_s = R_e + H$, R_e is the earth radius, and $\psi_k = \sin^{-1}\left(\frac{R_s}{R_e}\sin\vartheta_k\right) - \vartheta_k$ is the earth central angle of UT k [15]. In addition, the elevation angle of UT k can be computed by $\varepsilon_k = \cos^{-1}\left(\frac{R_s}{R_e}\sin\vartheta_k\right) \in [35.12°, 90°]$ [15]. The average channel power is calculated by $\beta_k = G_{\rm sat}G_{\rm ut}NM \cdot \lambda^2/(4\pi D_k)^2$, where $G_{\rm sat}$ and $G_{\rm ut}$ are the gains of antenna elements at the satellite and UTs, respectively. The random vector $\mathbf{d}_k = \sqrt{\frac{\kappa_k\beta_k}{\kappa_k+1}}\mathbf{d}_{k,0} + \sqrt{\frac{\beta_k}{\kappa_k+1}}\tilde{\mathbf{d}}_k$ in (7) is simulated in terms of $\mathbf{d}_k(t, f)$ in (6), where the first path is used to produce the LoS direction $\mathbf{d}_{k,0} = \mathbf{d}(\boldsymbol{\varphi}_{k,0})$ and the last $L_k - 1$ paths are used for $\tilde{\mathbf{d}}_k$. In this paper, we make $\boldsymbol{\varphi}_{k,0}$ to satisfy $\sin\varphi_{k,0}^{\rm y'} \sin\varphi_{k,0}^{\rm x'} = \sin\varepsilon_k$ (e.g., $\varphi_{k,0}^{\rm x'} = 90°$ and $\varphi_{k,0}^{\rm y'} = \varepsilon_k$) for simplicity, which means that each UT's UPA is placed horizontally. To generate $\tilde{\mathbf{d}}_k$, the path gains $\{a_{k,\ell}\}_{\ell=1}^{L_k-1}$ and paired AoAs $\{\boldsymbol{\varphi}_{k,\ell}\}_{\ell=1}^{L_k-1}$ are produced according to the exponential power delay spectrum and wrapped Gaussian power angle spectrum, respectively [2]. The noise variance is $\sigma_k^2 = k_{\rm B}T_{\rm n}B$ where $k_{\rm B} = 1.38 \times 10^{-23}$ J $\cdot$ K^{-1} is the Boltzmann constant, $T_{\rm n}$ is the noise temperature and B is the system bandwidth.

In Fig. 4, the sum rate performance for Algorithms 1–3 is depicted. Meanwhile, the per-

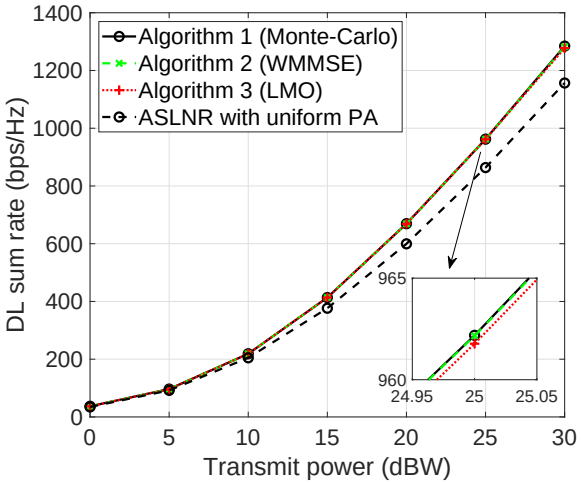

Fig. 4: DL sum rate performance of Algorithms 1–3.

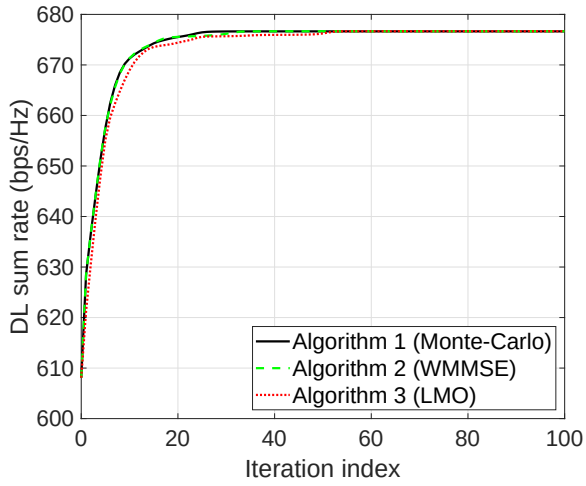

Fig. 5: Convergence of Algorithms 1–3 for $P = 20$ dBW.

formance of ASLNR precoders $\{\mathbf{w}_k^{\text{aslnr}}\}_{k=1}^K$ is also illustrated, where $\mathbf{w}_k^{\text{aslnr}} = \sqrt{p_k} \cdot \frac{\mathbf{T}_k^{-1}\mathbf{g}_k}{\|\mathbf{T}_k^{-1}\mathbf{g}_k\|}$ with $\mathbf{T}_k = \sum_{i=1}^K \beta_i \mathbf{g}_i \mathbf{g}_i^H + \frac{\sigma_k^2}{p_k}\mathbf{I}_M$ [37]. The power p_k of ASLNR precoder $\mathbf{w}_k^{\text{aslnr}}$ is set to be $p_k = P/K (\forall k \in \mathcal{K})$ for simplicity. It can be observed that the difference of sum rate performance among Algorithms 1–3 is negligible, and they have the performance gain of about 2 dB compared with the ASLNR precoders at $P = 25$ dBW. Algorithms 2 and 3 behave slightly worse than Algorithm 1 because of using the upper bound of ergodic sum rate. Nevertheless, Algorithm 3 can achieve approximately the same performance with Algorithms 1 and 2, even with much less computation effort.

In Fig. 5, we show the convergence performance for Algorithms 1–3. It is observed that Algorithms 1–3 will definitely converge within tens of iterations. The objective values attained by Algorithms 1–3 coincide with each other. Since the inner iterations in Algorithm 3 are only

carried out for scalar variables, the computation complexity of Algorithm 3 is much lower than that of Algorithms 1 and 2, which makes it to be a suitable option for precoding in massive MIMO LEO SATCOM. Moreover, as the precoder designs only rely on the sCSI, which is independent of subcarriers and time instances within a sCSI stable time-frequency resource block, the implementation overhead could be very low.

VI. Conclusion

In this paper, we have investigated the DL transmit design in FFR massive MIMO LEO SATCOM. First, we established the massive MIMO LEO satellite channel model, and the Doppler and delay were compensated for at each UT to simplify DL transmission. Then, we showed that the rank of transmit covariance matrix should not be larger than one to maximize ergodic sum rate, which indicated that precoding with at most one data stream for each UT is optimal for linear transmitters. The MM algorithm combined with Monte-Carlo method was used to solve the precoder design. To avoid the time-consuming sample average in Monte-Carlo method, we simplified the DL transmit design by approximating the DL ergodic rate with its closed-form upper bound. It was shown that the transmit covariance matrices keep the rank-one property, and the corresponding simplified precoder design was formulated. We derive the solution structure for the simplified precoder design, in which the precoders are determined by Lagrange multipliers. Then, an LMO problem is formulated, which has only one scalar to be optimized for each UT, and a low-complexity algorithm was proposed to solve the LMO problem. The convergence and performance of the proposed approaches were demonstrated in simulation results.

Appendix A
Proof of Proposition 1

Our proof shares the similar spirit with the approaches in [51]. We first prove that the optimal solution to $\mathcal{P}$ must be rank-one. Then, the proof procedures can be directly applied to the optimal solution to $\mathcal{P}^{\mathrm{ub}}$. The gradient of $\mathcal{R}_i$ with respect to $\mathbf{Q}_k$ can be calculated by

$$\frac{\partial \mathcal{R}_i}{\partial \mathbf{Q}_k^*} = \begin{cases} \frac{1}{\ln 2} \cdot \mathbb{E}\left\{ \frac{\|\mathbf{d}_k\|^2}{T_k(\mathbf{d}_k)} \right\} \mathbf{g}_k \mathbf{g}_k^H, & \text{if } i = k \\ \frac{1}{\ln 2} \cdot \left(\mathbb{E}\left\{ \frac{\|\mathbf{d}_i\|^2}{T_i(\mathbf{d}_i)} \right\} - \mathbb{E}\left\{ \frac{\|\mathbf{d}_i\|^2}{I_i(\mathbf{d}_i)} \right\} \right) \mathbf{g}_i \mathbf{g}_i^H, & \text{if } i \neq k \end{cases}, \tag{54}$$

where $T_k(\mathbf{d}_k) = \sigma_k^2 + \sum_{\ell=1}^{K} \mathbf{g}_k^H \mathbf{Q}_\ell \mathbf{g}_k \|\mathbf{d}_k\|^2$ and $I_k(\mathbf{d}_k) = \sigma_k^2 + \sum_{\ell \neq k} \mathbf{g}_k^H \mathbf{Q}_\ell \mathbf{g}_k \|\mathbf{d}_k\|^2$. The Lagrangian of $\mathcal{P}$ is given by

$$\mathcal{L}_{\mathcal{P}} = \sum_{k=1}^{K} \mathcal{R}_k - v \left(\sum_{k=1}^{K} \mathrm{tr}\left(\mathbf{Q}_k\right) - P \right) + \sum_{k=1}^{K} \mathrm{tr}\left(\mathbf{\Phi}_k \mathbf{Q}_k\right), \tag{55}$$

where $v \geq 0$ and $\mathbf{\Phi}_k \succeq \mathbf{0}$ are the Lagrange multipliers associated with the power constraint $\sum_{k=1}^{K} \mathrm{tr}\left(\mathbf{Q}_k\right) \leq P$ and positive semidefinite condition $\mathbf{Q}_k \succeq \mathbf{0}$. From the Karush-Kuhn-Tucker (KKT) conditions, the gradient of $\mathcal{L}_{\mathcal{P}}$ with respect to the optimal $\mathbf{Q}_k$ should be zero, i.e.,

$$\frac{\partial \mathcal{L}_{\mathcal{P}}}{\partial \mathbf{Q}_k^*} = -\mathbf{A}_k + \mathbf{B}_k - v\mathbf{I}_M + \mathbf{\Phi}_k = \mathbf{0}, \tag{56}$$

where $\mathbf{A}_k = \frac{1}{\ln 2} \cdot \sum_{i \neq k} \left(\mathbb{E}\left\{ \frac{\|\mathbf{d}_i\|^2}{I_i(\mathbf{d}_i)} \right\} - \mathbb{E}\left\{ \frac{\|\mathbf{d}_i\|^2}{T_i(\mathbf{d}_i)} \right\} \right) \mathbf{g}_i \mathbf{g}_i^H$ and $\mathbf{B}_k = \frac{1}{\ln 2} \cdot \mathbb{E}\left\{ \frac{\|\mathbf{d}_k\|^2}{T_k(\mathbf{d}_k)} \right\} \mathbf{g}_k \mathbf{g}_k^H$ are both positive semidefinite matrices. From (56), $\mathbf{\Phi}_k$ can be expressed as $\mathbf{\Phi}_k = v\mathbf{I}_M + \mathbf{A}_k - \mathbf{B}_k$. To guarantee $\mathbf{\Phi}_k \succeq \mathbf{0}$, we must have $v > 0$. Thus, we have $\mathrm{rank}(v\mathbf{I}_M + \mathbf{A}_k) = M$. From the rank-sum inequality $\left|\mathrm{rank}(\mathbf{A}) - \mathrm{rank}(\mathbf{B})\right| \leq \mathrm{rank}(\mathbf{A} + \mathbf{B})$ [41, 0.4.5(d)], the rank of $\mathbf{\Phi}_k$ must satisfy $\mathrm{rank}(\mathbf{\Phi}_k) \geq M - 1$. Due to the Sylvester inequality $\mathrm{rank}(\mathbf{A}) + \mathrm{rank}(\mathbf{B}) - n \leq \mathrm{rank}(\mathbf{AB})$ [41, 0.4.5(c)], where n is the column number of $\mathbf{A}$, we can obtain

$$\mathrm{rank}(\mathbf{\Phi}_k) + \mathrm{rank}(\mathbf{Q}_k) - M \leq \mathrm{rank}(\mathbf{\Phi}_k \mathbf{Q}_k) \overset{\text{(a)}}{=} 0, \tag{57}$$

where (a) follows from the complementary slackness condition $\mathbf{\Phi}_k \mathbf{Q}_k = \mathbf{0}$. The rank of $\mathbf{Q}_k$ will satisfy $\mathrm{rank}(\mathbf{Q}_k) \leq 1$. This concludes the proof.

APPENDIX B
A MINORIZING FUNCTION OF $\mathcal{R}_k$

Let $\mathbf{W}^{(n)} = \left[\mathbf{w}_1^{(n)} \ldots \mathbf{w}_K^{(n)} \right]$ be the collection of precoding vectors in the nth iteration. The MMSE in the nth iteration is given by $\mathrm{MMSE}_k^{(n)} = 1 - \frac{|\mathbf{g}_k^H \mathbf{w}_k^{(n)}|^2 \|\mathbf{d}_k\|^2}{\sigma_k^2 + \sum_{i=1}^{K} |\mathbf{g}_k^H \mathbf{w}_i^{(n)}|^2 \|\mathbf{d}_k\|^2}$. From the concavity of $\log_2(\cdot)$, we have

$$\begin{aligned} \mathcal{R}_k &= -\mathbb{E}\left\{\log_2 \mathrm{MMSE}_k\right\} \geq \mathcal{R}_k^{(n)} - \frac{1}{\ln 2} \cdot \mathbb{E}\left\{ \frac{\mathrm{MMSE}_k - \mathrm{MMSE}_k^{(n)}}{\mathrm{MMSE}_k^{(n)}} \right\} \\ &\overset{\text{(a)}}{\geq} \mathcal{R}_k^{(n)} + \frac{1}{\ln 2} - \frac{1}{\ln 2} \cdot \mathbb{E}\left\{ \frac{\mathrm{MSE}_k}{\mathrm{MMSE}_k^{(n)}} \right\} \triangleq g_k^{(n)}, \end{aligned} \tag{58}$$

where $\mathcal{R}_k^{(n)}$ is the DL ergodic rate of UT k in the nth iteration, (a) follows from $\mathrm{MMSE}_k \leq \mathrm{MSE}_k$. As indicated in (18), MSE_k is a function of precoder $\mathbf{W}$ and receiver $\mathbf{c}_k$. If the inequality

$\mathcal{R}_k \geq g_k^{(n)}$ in (58) holds with equality at $\mathbf{W}^{(n)}$, the receiver $\mathbf{c}_k$ in MSE_k should be given by $\mathbf{c}_k^{(n)} = \frac{\mathbf{d}_k \cdot \mathbf{g}_k^H \mathbf{w}_k^{(n)}}{\sigma_k^2 + \sum_{i=1}^K |\mathbf{g}_k^H \mathbf{w}_i^{(n)}|^2 \|\mathbf{d}_k\|^2}$. After substituting $\mathbf{c}_k^{(n)}$ into MSE_k, we have

$$\mathbb{E}\left\{\frac{\mathrm{MSE}_k}{\mathrm{MMSE}_k^{(n)}}\right\} = a_k^{(n)} \sum_{i=1}^K |\mathbf{w}_i^H \mathbf{g}_k|^2 - 2\Re\left\{\mathbf{w}_k^H \mathbf{g}_k \cdot b_k^{(n)}\right\} + c_k^{(n)}, \tag{59}$$

where $a_k^{(n)} = \mathbb{E}\left\{\frac{|\mathbf{d}_k^H \mathbf{c}_k^{(n)}|^2}{\mathrm{MMSE}_k^{(n)}}\right\}$, $b_k^{(n)} = \mathbb{E}\left\{\frac{\mathbf{d}_k^H \mathbf{c}_k^{(n)}}{\mathrm{MMSE}_k^{(n)}}\right\}$ and $c_k^{(n)} = \mathbb{E}\left\{\frac{\sigma_k^2 \|\mathbf{c}_k^{(n)}\|^2 + 1}{\mathrm{MMSE}_k^{(n)}}\right\}$.

APPENDIX C
PROOF OF PROPOSITION 2

The Lagrangian of (31) is given by

$$\mathcal{L}_{\mathcal{Q}}^{\mathrm{ub}} = \sum_{k=1}^K \|\mathbf{w}_k\|^2 + \sum_{k=1}^K \lambda_k \left(\frac{\beta_k}{\sigma_k^2} \sum_{i \neq k} |\mathbf{w}_i^H \mathbf{g}_k|^2 + 1 - \frac{\beta_k}{\gamma_k \sigma_k^2} |\mathbf{w}_k^H \mathbf{g}_k|^2\right), \tag{60}$$

where $\lambda_k \geq 0$ is the Lagrange multiplier associated with the inequality for UT k in (31). The gradient of $\mathcal{L}_{\mathcal{Q}}^{\mathrm{ub}}$ can be written as

$$\frac{\partial \mathcal{L}_{\mathcal{Q}}^{\mathrm{ub}}}{\partial \mathbf{w}_k^*} = \mathbf{w}_k + \sum_{i \neq k} \frac{\lambda_i \beta_i}{\sigma_i^2} \mathbf{g}_i \mathbf{g}_i^H \mathbf{w}_k - \frac{\lambda_k \beta_k}{\gamma_k \sigma_k^2} \mathbf{g}_k \mathbf{g}_k^H \mathbf{w}_k. \tag{61}$$

By setting the gradient of $\mathcal{L}_{\mathcal{Q}}^{\mathrm{ub}}$ as zero, we can obtain the condition that the minimizer of $\mathcal{L}_{\mathcal{Q}}^{\mathrm{ub}}$ satisfies as follows

$$\left(\sum_{i \neq k} \frac{\lambda_i \beta_i}{\sigma_i^2} \mathbf{g}_i \mathbf{g}_i^H + \mathbf{I}_M\right) \mathbf{w}_k = \frac{\lambda_k \beta_k}{\gamma_k \sigma_k^2} \mathbf{g}_k \mathbf{g}_k^H \mathbf{w}_k, \tag{62}$$

which is equivalent to (33) actually. Substituting (62) into (60) yields the minimum of $\mathcal{L}_{\mathcal{Q}}^{\mathrm{ub}}$ as $\sum_{k=1}^K \lambda_k$. As stated in Section IV-B, when r_k is the optimal $\mathcal{R}_k^{\mathrm{ub}}$ in $\mathcal{S}^{\mathrm{ub}}$, the optimal value of $\mathcal{Q}^{\mathrm{ub}}$ is P. Because the duality gap for the problem $\mathcal{Q}^{\mathrm{ub}}$ is zero, which can be easily verified by using the approaches in [47], [52], the optimal Lagrange multipliers $\{\lambda_k\}_{k=1}^K$ of (31) must satisfy $\sum_{k=1}^K \lambda_k = P$. This concludes the proof.

APPENDIX D
PROOF OF PROPOSITION 3

The optimal DL precoder to $\mathcal{S}^{\mathrm{ub}}$ must satisfy the power constraint with equality, because any precoders with $\sum_{k=1}^K \|\mathbf{w}_k\|^2 < P$ can be scaled up to increase the objective value. Suppose that $\{\mathbf{w}_k^\circ\}_{k=1}^K$ is a feasible solution to $\mathcal{S}^{\mathrm{ub}}$ satisfying $\sum_{k=1}^K \left\|\mathbf{w}_k^\circ\right\|^2 = P$. Let r_k° represent the rate of UT k by substituting $\{\mathbf{w}_k^\circ\}_{k=1}^K$ into (27), and denote $\gamma_k^\circ = 2^{r_k^\circ} - 1$. We can calculate the Lagrange

multipliers $\{\lambda_k^\circ\}_{k=1}^K$ by solving $\mathcal{Q}^{\rm ub}$ in (31) where the thresholds are chosen as $\{\gamma_k^\circ\}_{k=1}^K$. Then, $\{\mathbf{w}_k^\circ\}_{k=1}^K$ and $\{\lambda_k^\circ\}_{k=1}^K$ will satisfy the KKT condition of $\mathcal{Q}^{\rm ub}$ in (31) for thresholds being $\{\gamma_k^\circ\}_{k=1}^K$. Therefore, the Lagrange multipliers will satisfy $\sum_{k=1}^K \lambda_k^\circ = P$, which implies that $\{\lambda_k^\circ\}_{k=1}^K$ is a feasible solution to $\mathcal{M}^{\rm ub}$. In addition, the objective value of $\mathcal{M}^{\rm ub}$ attained by $\{\lambda_k^\circ\}_{k=1}^K$ will be $\sum_{k=1}^K r_k^\circ$.

On the other hand, let $\{\lambda_k^\diamond\}_{k=1}^K$ be a feasible solution to $\mathcal{M}^{\rm ub}$, i.e., $\sum_{k=1}^K \lambda_k^\diamond = P$. Then, $r_k^\diamond$ is calculated by substituting $\{\lambda_k^\diamond\}_{k=1}^K$ into (38), and denote $\gamma_k^\diamond = 2^{r_k^\diamond} - 1$. We can calculate DL precoders $\{\mathbf{w}_k^\diamond\}_{k=1}^K$ via (34) and (36) where thresholds are equal to $\{\gamma_k^\diamond\}_{k=1}^K$. Now, $\{\mathbf{w}_k^\diamond\}_{k=1}^K$ and $\{\lambda_k^\diamond\}_{k=1}^K$ will satisfy the KKT condition of $\mathcal{Q}^{\rm ub}$ in (31) with thresholds $\{\gamma_k^\diamond\}_{k=1}^K$. Therefore, $\{\mathbf{w}_k^\diamond\}_{k=1}^K$ will satisfy $\sum_{k=1}^K \left\|\mathbf{w}_k^\diamond\right\|^2 = P$, which means that $\{\mathbf{w}_k^\diamond\}_{k=1}^K$ is a feasible solution to $\mathcal{S}^{\rm ub}$. Furthermore, $\{\mathbf{w}_k^\diamond\}_{k=1}^K$ can achieve the objective value $\sum_{k=1}^K r_k^\diamond$ for problem $\mathcal{S}^{\rm ub}$.

Combining the above results, we can conclude that $\mathcal{M}^{\rm ub}$ and $\mathcal{S}^{\rm ub}$ have the same objective value region, and also the optimal value. This concludes the proof.

APPENDIX E
A MINORIZING FUNCTION OF r_k

Define the $\mathrm{VMMSE}_k^{(n)} = 1 - \frac{\lambda_k^{(n)}\beta_k}{\sigma_k^2}\mathbf{g}_k^H \left(\sum_{i=1}^K \frac{\lambda_i^{(n)}\beta_i}{\sigma_i^2}\mathbf{g}_i\mathbf{g}_i^H + \mathbf{I}_M\right)^{-1}\mathbf{g}_k$ as the VMMSE of UT k in the nth iteration. By applying the concavity of $\log_2(\cdot)$, we have

$$\begin{aligned} r_k = -\log_2 \mathrm{VMMSE}_k &\geq r_k^{(n)} - \frac{1}{\ln 2}\frac{\mathrm{VMMSE}_k - \mathrm{VMMSE}_k^{(n)}}{\mathrm{VMMSE}_k^{(n)}} \\ &\overset{\text{(a)}}{\geq} r_k^{(n)} + \frac{1}{\ln 2} - \frac{1}{\ln 2}\frac{\mathrm{VMSE}_k}{\mathrm{VMMSE}_k^{(n)}} \triangleq h_k^{(n)}, \end{aligned} \tag{63}$$

where $r_k^{(n)}$ is the r_k in the nth iteration, (a) follows from $\mathrm{VMMSE}_k \leq \mathrm{VMSE}_k$. Notice that VMSE_k in (42) is relevant to $\{\lambda_k\}_{k=1}^K$ and $\mathbf{u}_k$. To make the last inequality in (63) holds with equality, we choose $\mathbf{u}_k$ in VMSE_k to be $\mathbf{u}_k^{(n)} = \left(\sum_{i=1}^K \frac{\lambda_i^{(n)}\beta_i}{\sigma_i^2}\mathbf{g}_i\mathbf{g}_i^H + \mathbf{I}_M\right)^{-1}\mathbf{g}_k\sqrt{\frac{\lambda_k^{(n)}\beta_k}{\sigma_k^2}}$. Substituting $\mathbf{u}_k^{(n)}$ into VMSE_k yields

$$\frac{\mathrm{VMSE}_k}{\mathrm{VMMSE}_k^{(n)}} = \sum_{i=1}^K \psi_{k,i}^{(n)}\frac{\lambda_i\beta_i}{\sigma_i^2} - 2\chi_k^{(n)}\sqrt{\frac{\lambda_k\beta_k}{\sigma_k^2}} + \delta_k^{(n)}, \tag{64}$$

where $\psi_{k,i}^{(n)} = \frac{|\mathbf{g}_i^H\mathbf{u}_k^{(n)}|^2}{\mathrm{VMMSE}_k^{(n)}}$, $\chi_k^{(n)} = \frac{\Re\{\mathbf{g}_k^H\mathbf{u}_k^{(n)}\}}{\mathrm{VMMSE}_k^{(n)}}$ and $\delta_k^{(n)} = \frac{\|\mathbf{u}_k^{(n)}\|^2+1}{\mathrm{VMMSE}_k^{(n)}}$.

APPENDIX F
PROOF OF PROPOSITION 4

The sum of r_k can be written as

$$\sum_{k=1}^{K} r_k = -\sum_{k=1}^{K} \log_2 \left[\left(\mathbf{I} + \mathbf{\Gamma}^{\frac{1}{2}} \mathbf{G}^H \mathbf{G} \mathbf{\Gamma}^{\frac{1}{2}} \right)^{-1} \right]_{k,k} = -\log_2 \prod_{k=1}^{K} \left[\left(\mathbf{I} + \mathbf{\Gamma}^{\frac{1}{2}} \mathbf{G}^H \mathbf{G} \mathbf{\Gamma}^{\frac{1}{2}} \right)^{-1} \right]_{k,k}$$
$$\overset{\text{(a)}}{\leq} \log_2 \det \left(\mathbf{I} + \mathbf{\Gamma}^{\frac{1}{2}} \mathbf{G}^H \mathbf{G} \mathbf{\Gamma}^{\frac{1}{2}} \right) \overset{\text{(b)}}{\leq} \log_2 \prod_{k=1}^{K} \left[\mathbf{I} + \mathbf{\Gamma}^{\frac{1}{2}} \mathbf{G}^H \mathbf{G} \mathbf{\Gamma}^{\frac{1}{2}} \right]_{k,k} = \sum_{k=1}^{K} \log_2 \left(1 + \frac{\lambda_k \beta_k}{\sigma_k^2} \right), \quad (65)$$

where (a) and (b) follow from the Hadamard's inequality $\det \mathbf{A} \leq \prod_{k=1}^{K} [\mathbf{A}]_{k,k}$ [41], and the equality holds if and only if $\mathbf{\Gamma}^{\frac{1}{2}} \mathbf{G}^H \mathbf{G} \mathbf{\Gamma}^{\frac{1}{2}}$ is diagonal. Since $\mathbf{\Gamma}$ is diagonal, $\mathbf{\Gamma}^{\frac{1}{2}} \mathbf{G}^H \mathbf{G} \mathbf{\Gamma}^{\frac{1}{2}}$ is diagonal, if and only if $\mathbf{G}^H \mathbf{G}$ is diagonal, which also means $\mathbf{G}^H \mathbf{G} = \mathbf{I}$. This concludes the proof.

REFERENCES

[1] A. Guidotti, A. Vanelli-Coralli, M. Conti, S. Andrenacci, S. Chatzinotas, N. Maturo, B. Evans, A. Awoseyila, A. Ugolini, T. Foggi, L. Gaudio, N. Alagha, and S. Cioni, "Architectures and key technical challenges for 5G systems incorporating satellites," *IEEE Trans. Veh. Technol.*, vol. 68, no. 3, pp. 2624–2639, Mar. 2019.

[2] 3GPP TR 38.811, "Study on new radio (NR) to support non-terrestrial networks (Release 15)," Sophia Antipolis Valbonne, France, V15.3.0, Jul. 2020.

[3] Z. Qu, G. Zhang, H. Cao, and J. Xie, "LEO satellite constellation for Internet of Things," *IEEE Access*, vol. 5, pp. 18 391–18 401, 2017.

[4] A. Guidotti, A. Vanelli-Coralli, T. Foggi, G. Colavolpe, M. Caus, J. Bas, S. Cioni, and A. Modenini, "LTE-based satellite communications in LEO mega-constellations," *Int. J. Satell. Commun. Netw.*, vol. 37, no. 4, pp. 316–330, Jun. 2019.

[5] B. Di, L. Song, Y. Li, and H. V. Poor, "Ultra-dense LEO: Integration of satellite access networks into 5G and beyond," *IEEE Wireless Commun.*, vol. 26, no. 2, pp. 62–69, Apr. 2019.

[6] Y. Su, Y. Liu, Y. Zhou, J. Yuan, H. Cao, and J. Shi, "Broadband LEO satellite communications: Architectures and key technologies," *IEEE Wireless Commun.*, vol. 26, no. 2, pp. 55–61, Apr. 2019.

[7] I. del Portillo, B. G. Cameron, and E. F. Crawley, "A technical comparison of three low earth orbit satellite constellation systems to provide global broadband," *Acta Astronautica*, vol. 159, pp. 123–135, 2019.

[8] P.-D. Arapoglou, K. Liolis, M. Bertinelli, A. Panagopoulos, P. Cottis, and R. De Gaudenzi, "MIMO over satellite: A review," *IEEE Commun. Surveys Tuts.*, vol. 13, no. 1, pp. 27–51, 2011.

[9] P.-D. Arapoglou, P. Burzigotti, M. Bertinelli, A. B. Alamanac, and R. De Gaudenzi, "To MIMO or not to MIMO in mobile satellite broadcasting systems," *IEEE Trans. Wireless Commun.*, vol. 10, no. 9, pp. 2807–2811, Sep. 2011.

[10] A. Byman, A. Hulkkonen, P.-D. Arapoglou, M. Bertinelli, and R. De Gaudenzi, "MIMO for mobile satellite digital broadcasting: From theory to practice," *IEEE Trans. Veh. Technol.*, vol. 65, no. 7, pp. 4839–4853, Jul. 2016.

[11] R. T. Schwarz, T. Delamotte, K.-U. Storek, and A. Knopp, "MIMO applications for multibeam satellites," *IEEE Trans. Broadcast.*, vol. 65, no. 4, pp. 664–681, Dec. 2019.

[12] C. A. Hofmann, R. T. Schwarz, and A. Knopp, "Multisatellite UHF MIMO channel measurements," *IEEE Antennas Wireless Propag. Lett.*, vol. 16, pp. 2481–2484, 2017.

[13] G. Maral and M. Bousquet, *Satellite Communications Systems: Systems, Techniques and Technology*, 5th ed. Chichester, UK: Wiley, 2009.

[14] W. Hong, Z. H. Jiang, C. Yu, J. Zhou, P. Chen, Z. Yu, H. Zhang, B. Yang, X. Pang, M. Jiang, Y. Cheng, M. K. T. Al-Nuaimi, Y. Zhang, J. Chen, and S. He, "Multibeam antenna technologies for 5G wireless communications," *IEEE Trans. Antennas Propag.*, vol. 65, no. 12, pp. 6231–6249, Dec. 2017.

[15] E. Lutz, M. Werner, and A. Jahn, *Satellite Systems for Personal and Broadband Communications*. Berlin, Heidelberg: Springer, 2000.

[16] M. Schneider, C. Hartwanger, and H. Wolf, "Antennas for multiple spot beam satellites," *CEAS Space J.*, vol. 2, no. 1, pp. 59–66, Dec. 2011.

[17] P. L. Metzen, "Globalstar satellite phased array antennas," in *Proc. IEEE ICPAST*, Dana Point, CA, USA, May 2000, pp. 207–210.

[18] H. Fenech, A. Tomatis, S. Amos, V. Soumpholphakdy, and J. L. S. Merino, "Eutelsat HTS systems," *Int. J. Satell. Commun. Netw.*, vol. 34, no. 4, pp. 503–521, Jan. 2016.

[19] M. A. Vázquez, A. Pérez-Neira, D. Christopoulos, S. Chatzinotas, B. Ottersten, P.-D. Arapoglou, A. Ginesi, and G. Tarocco, "Precoding in multibeam satellite communications: Present and future challenges," *IEEE Wireless Commun.*, vol. 23, no. 6, pp. 88–95, Dec. 2016.

[20] A. I. Pérez-Neira, M. A. Vázquez, M. R. B. Shankar, S. Maleki, and S. Chatzinotas, "Signal processing for high-throughput satellites: Challenges in new interference-limited scenarios," *IEEE Signal Process. Mag.*, vol. 36, no. 4, pp. 112–131, Jul. 2019.

[21] G. Zheng, S. Chatzinotas, and B. Ottersten, "Generic optimization of linear precoding in multibeam satellite systems," *IEEE Trans. Wireless Commun.*, vol. 11, no. 6, pp. 2308–2320, Jun. 2012.

[22] D. Christopoulos, S. Chatzinotas, and B. Ottersten, "Multicast multigroup precoding and user scheduling for frame-based satellite communications," *IEEE Trans. Wireless Commun.*, vol. 14, no. 9, pp. 4695–4707, Sep. 2015.

[23] V. Joroughi, M. A. Vázquez, and A. I. Pérez-Neira, "Precoding in multigateway multibeam satellite systems," *IEEE Trans. Wireless Commun.*, vol. 15, no. 7, pp. 4944–4956, Jul. 2016.

[24] C. Mosquera, R. López-Valcarce, T. Ramírez, and V. Joroughi, "Distributed precoding systems in multi-gateway multibeam satellites: Regularization and coarse beamforming," *IEEE Trans. Wireless Commun.*, vol. 17, no. 10, pp. 6389–6403, Oct. 2018.

[25] W. Wang, A. Liu, Q. Zhang, L. You, X. Q. Gao, and G. Zheng, "Robust multigroup multicast transmission for frame-based multi-beam satellite systems," *IEEE Access*, vol. 6, pp. 46 074–46 083, 2018.

[26] J. Wang, L. Zhou, K. Yang, X. Wang, and Y. Liu, "Multicast precoding for multigateway multibeam satellite systems with feeder link interference," *IEEE Trans. Wireless Commun.*, vol. 18, no. 3, pp. 1637–1650, Mar. 2019.

[27] Z. Lin, M. Lin, Y. Huang, T. de Cola, and W.-P. Zhu, "Robust multi-objective beamforming for integrated satellite and high altitude platform network with imperfect channel state information," *IEEE Trans. Signal Process.*, vol. 67, no. 24, pp. 6384–6396, Dec. 2019.

[28] X. Q. Gao, B. Jiang, X. Li, A. B. Gershman, and M. R. McKay, "Statistical eigenmode transmission over jointly correlated MIMO channels," *IEEE Trans. Inf. Theory*, vol. 55, no. 8, pp. 3735–3750, Aug. 2009.

[29] S. Jarmyr, B. Ottersten, and E. A. Jorswieck, "Statistical precoding with decision feedback equalization over a correlated MIMO channel," *IEEE Trans. Signal Process.*, vol. 58, no. 12, pp. 6298–6311, Dec. 2010.

[30] T. L. Marzetta, "Noncooperative cellular wireless with unlimited numbers of base station antennas," *IEEE Trans. Wireless Commun.*, vol. 9, no. 11, pp. 3590–3600, Nov. 2010.

[31] H. Q. Ngo, E. G. Larsson, and T. L. Marzetta, "Energy and spectral efficiency of very large multiuser MIMO systems," *IEEE Trans. Commun.*, vol. 61, no. 4, pp. 1436–1449, Apr. 2013.

[32] R. De Gaudenzi, P. Angeletti, D. Petrolati, and E. Re, "Future technologies for very high throughput satellite systems," *Int. J. Satell. Commun. Netw.*, pp. 1–21, Jul. 2019.

[33] P. Angeletti and R. De Gaudenzi, "A pragmatic approach to massive MIMO for broadband communication satellites," *IEEE Access*, vol. 8, pp. 132 212–132 236, 2020.

[34] A. Adhikary, J. Nam, J. Ahn, and G. Caire, "Joint spatial division and multiplexing – The large-scale array regime," *IEEE Trans. Inf. Theory*, vol. 59, no. 10, pp. 6441–6463, Oct. 2013.

[35] C. Sun, X. Q. Gao, S. Jin, M. Matthaiou, Z. Ding, and C. Xiao, "Beam division multiple access transmission for massive MIMO communications," *IEEE Trans. Commun.*, vol. 63, no. 6, pp. 2170–2184, Jun. 2015.

[36] A.-A. Lu, X. Q. Gao, W. Zhong, C. Xiao, and X. Meng, "Robust transmission for massive MIMO downlink with imperfect CSI," *IEEE Trans. Commun.*, vol. 67, no. 8, pp. 5362–5376, Aug. 2019.

[37] L. You, K.-X. Li, J. Wang, X. Q. Gao, X.-G. Xia, and B. Ottersten, "Massive MIMO transmission for LEO satellite communications," *IEEE J. Sel. Areas Commun.*, vol. 38, no. 8, pp. 1851–1865, Aug. 2020.

[38] I. Ali, N. Al-Dhahir, and J. E. Hershey, "Doppler characterization for LEO satellites," *IEEE Trans. Commun.*, vol. 46, no. 3, pp. 309–313, Mar. 1998.

[39] A. Papathanassiou, A. K. Salkintzis, and P. T. Mathiopoulos, "A comparison study of the uplink performance of W-CDMA and OFDM for mobile multimedia communications via LEO satellites," *IEEE Personal Communications*, vol. 8, no. 3, pp. 35–43, Jun. 2001.

[40] T. Hwang, C. Yang, G. Wu, S. Li, and G. Y. Li, "OFDM and its wireless applications: A survey," *IEEE Trans. Veh. Technol.*, vol. 58, no. 4, pp. 1673–1694, May 2009.

[41] R. A. Horn and C. R. Johnson, *Matrix Analysis*, 2nd ed. New York, NY, USA: Cambridge Univ. Press, 2013.

[42] R. A. Monzingo, R. L. Haupt, and T. W. Miller, *Introduction to Adaptive Arrays*, 2nd ed. New York, USA: Wiley, 2004.

[43] D. R. Hunter and K. Lange, "A tutorial on MM algorithms," *The American Statistician*, vol. 58, no. 1, pp. 30–37, 2004.

[44] S. Boyd and L. Vandenberghe, *Convex Optimization*. New York, NY, USA: Cambridge Univ. Press, 2004.

[45] M. D. Zoltowski, M. Haardt, and C. P. Mathews, "Closed-form 2-D angle estimation with rectangular arrays in element space or beamspace via unitary ESPRIT," *IEEE Trans. Signal Process.*, vol. 44, no. 2, pp. 316–328, Feb. 1996.

[46] Q. Shi, M. Razaviyayn, Z.-Q. Luo, and C. He, "An iteratively weighted MMSE approach to distributed sum-utility maximization for a MIMO interfering broadcast channel," *IEEE Trans. Signal Process.*, vol. 59, no. 9, pp. 4331–4340, Sep. 2011.

[47] E. Björnson, M. Bengtsson, and B. Ottersten, "Optimal multiuser transmit beamforming: A difficult problem with a simple solution structure [lecture notes]," *IEEE Signal Process. Mag.*, vol. 31, no. 4, pp. 142–148, Jul. 2014.

[48] A. Wiesel, Y. C. Eldar, and S. Shamai, "Linear precoding via conic optimization for fixed MIMO receivers," *IEEE Trans. Signal Process.*, vol. 54, no. 1, pp. 161–176, Jan. 2006.

[49] T. M. Cover and J. A. Thomas, *Elements of Information Theory*, 2nd ed. New Jersey, USA: Wiley, 2006.

[50] A. W. Rudge, K. Milne, A. D. Olver, and P. Knight, *Handbook of Antenna Design, Vol. 2*. London, UK: Peter Peregrinus Ltd., 1983.

[51] C. Sun, X. Q. Gao, J. Wang, Z. Ding, and X.-G. Xia, "Beam domain massive MIMO for optical wireless communications with transmit lens," *IEEE Trans. Commun.*, vol. 67, no. 3, pp. 2188–2202, Mar. 2019.

[52] W. Yu and T. Lan, "Transmitter optimization for the multi-antenna downlink with per-antenna power constraints," *IEEE Trans. Signal Process.*, vol. 55, no. 6, pp. 2646–2660, Jun. 2007.